Zirconium Bisamidinate Complexes with Sterically Demanding Ligands: Structure, Solution Dynamics, and Reactivity

Edwin Otten, Peter Dijkstra, Cindy Visser, Auke Meetsma, and Bart Hessen*

Stratingh Institute for Chemistry and Chemical Engineering, Center for Catalytic Olefin Polymerization, University of Groningen, Nijenborgh 4, NL-9747 AG Groningen, The Netherlands

Received May 2, 2005

Bisamidinate zirconium dichloride and dimethyl complexes with the sterically demanding amidinate ligands $[PhC(NAr)_2)]^-$ (**A**) and $[PhC(NAr)(NAr')]^-$ (**B**) (Ar = 2,6-^{i}Pr$_2$C$_6$H$_3$; Ar′ = 2,6-Me$_2$C$_6$H$_3$) were prepared. The steric demand of ligand **A** induces the unusual *trans* geometry in *trans*-(**A**)$_2$ZrCl$_2$, whereas (**A**)$_2$ZrMe$_2$ and (**B**)$_2$ZrX$_2$ (X = Cl, Me) adopt the more usual *cis*-X$_2$ geometry. The dynamic behavior of these complexes in solution was studied by 1D and 2D ^{1}H NMR spectroscopy. Reaction of (**A**)$_2$ZrMe$_2$ with H$_2$ leads, after stepwise hydrogenolysis of the Zr−Me bonds, to cyclometalation of the two amidinate ligands. The same product was obtained by thermolysis of the dimethyl complex. The square pyramidal five-coordinate 10 valence electron cationic monomethyl species $[(\mathbf{A})_2ZrMe]^+$ was generated and structurally characterized. Remarkably, the compound is unreactive toward ethylene, H$_2$, and CO. The sterically slightly less encumbered species $[(\mathbf{B})_2ZrMe]^+$ does polymerize ethylene, albeit with modest activity.

Introduction

In recent years, group 4 metal complexes supported by a wide variety of monoanionic bidentate ligand systems have been developed as model systems for the octahedral active site of Ziegler−Natta-type polymerization catalysts.[1] Among these ligands, amidinates are attractive due to their easy preparation, modifiability, and versatile coordination properties.[2] Monoamidinate,[3] mixed-ligand,[4] and bisamidinate compounds[5] of the group 4 metals have been studied as catalysts for the polymerization of various olefins. Due to the C_2 symmetric *cis*-octahedral structure that six-coordinate bisamidinate group 4 metal derivatives invariably adopt, they can be used for the stereoregular polymerization of α-olefins. Eisen and co-workers recently reported propylene polymerization studies with such complexes, in which they found the stereoregularity of the polymer to be modulated by propylene pressure.[6] Arnold and co-workers have focused on other types of reactivity with group 4 metal bisamidinate complexes, including the chemistry of low-valent derivatives.[7] The majority of these studies are based on complexes with the *N*,*N*′-bis(trimethylsilyl)benzamidinate ligand. Sterically more demanding *N*,*N*′-diarylbenzamidines $[RC(NAr)_2]H$ (R = Me, *p*-MeC$_6$H$_4$, *p*-MeOC$_6$H$_4$; Ar = 2,6-^{i}Pr$_2$C$_6$H$_3$) were first prepared by Boeré and co-workers.[8] The steric hindrance imparted by such ligands has allowed the isolation and characterization of metal complexes with unusual geometries. Recently, main group complexes of

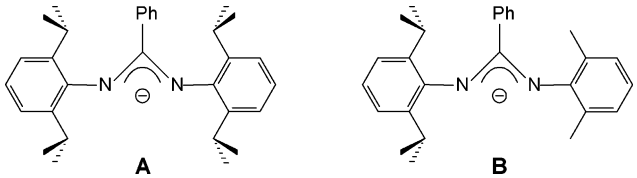

Figure 1.

* To whom correspondence should be addressed. E-mail: B.Hessen@rug.nl.

(1) (a) Britovsek, G. J. P.; Gibson, V. C.; Wass, D. F. *Angew. Chem., Int. Ed.* **1999**, *38*, 428. (b) Coates, G. W.; Hustad, P. D.; Reinartz, S. *Angew. Chem., Int. Ed.* **2002**, *41*, 2236. (c) Gibson, V. C.; Spitzmesser, S. K. *Chem. Rev.* **2003**, *103*, 283.

(2) (a) Barker, J.; Kilner, M. *Coord. Chem. Rev.* **1994**, *133*, 219. (b) Edelmann, F. T. *Coord. Chem. Rev.* **1994**, *137*, 403.

(3) (a) Flores, J. C.; Chien, J. C. W.; Rausch, M. D. *Organometallics* **1995**, *14*, 1827. (b) Averbuj, C.; Tish, E.; Eisen, M. S. *J. Am. Chem. Soc.* **1998**, *120*, 8640. (c) Flores, J. C.; Chien, J. C. W.; Rausch, M. D. *Organometallics* **1995**, *14*, 2106.

(4) (a) Sita, L. R.; Babcock, J. R. *Organometallics* **1998**, *17*, 5228. (b) Gómez, R.; Duchateau, R.; Chernega, A. N.; Teuben, J. H.; Edelmann, F. T.; Green, M. L. H. *J. Organomet. Chem.* **1995**, *491*, 153. (c) Gómez, R.; Duchateau, R.; Chernega, A. N.; Meetsma, A.; Edelmann, F. T.; Teuben, J. H.; Green, M. L. H. *J. Chem. Soc., Dalton Trans.* **1995**, 217. (d) Gómez, R.; Green, M. L. H.; Haggitt, J. L. *J. Chem. Soc., Dalton Trans.* **1996**, 939. (e) Koterwas, L. A.; Fettinger, J. C.; Sita, L. R. *Organometallics* **1999**, *18*, 4183. (f) Jayaratne, K. C.; Sita, L. R. *J. Am. Chem. Soc.* **2000**, *122*, 958. (g) Keaton, R. J.; Jayaratne, K. C.; Henningsen, D. A.; Koterwas, L. A.; Sita, L. R. *J. Am. Chem. Soc.* **2001**, *123*, 6197. (h) Zhang, Y. H.; Reeder, E. K.; Keaton, R. J.; Sita, L. R. *Organometallics* **2004**, *23*, 3512.

(5) (a) Herskovics-Korine, D.; Eisen, M. S. *J. Organomet. Chem.* **1995**, *503*, 307. (b) Walther, D.; Fischer, R.; Görls, H.; Koch, J.; Schweder, B. *J. Organomet. Chem.* **1996**, *508*, 13. (c) Richter, J.; Edelmann, F. T.; Noltemeyer, M.; Schmidt, H. G.; Shmulinson, M.; Eisen, M. S. *J. Mol. Catal. A* **1998**, *130*, 149. (d) Littke, A.; Sleiman, N.; Bensimon, C.; Richeson, D. S.; Yap, G. P. A.; Brown, S. J. *Organometallics* **1998**, *17*, 446.

(6) (a) Volkis, V.; Shmulinson, M.; Averbuj, C.; Lisovskii, A.; Edelmann, F. T.; Eisen, M. S. *Organometallics* **1998**, *17*, 3155. (b) Volkis, V.; Nelkenbaum, E.; Lisovskii, A.; Hasson, G.; Semiat, R.; Kapon, M.; Botoshansky, M.; Eishen, Y.; Eisen, M. S. *J. Am. Chem. Soc.* **2003**, *125*, 2179.

(7) (a) Hagadorn, J. R.; Arnold, J. *Organometallics* **1994**, *13*, 4670. (b) Hagadorn, J. R.; Arnold, J. *J. Am. Chem. Soc.* **1996**, *118*, 893. (c) Hagadorn, J. R.; Arnold, J. *J. Chem. Soc., Dalton Trans.* **1997**, 3087. (d) Hagadorn, J. R.; Arnold, J. *Organometallics* **1998**, *17*, 1355.

(8) Boeré, R. T.; Klassen, V.; Wolmershäuser, G. *J. Chem. Soc., Dalton Trans.* **1998**, 4147.

10.1021/om050342j CCC: $30.25
Publication on Web 07/28/2005

Scheme 1

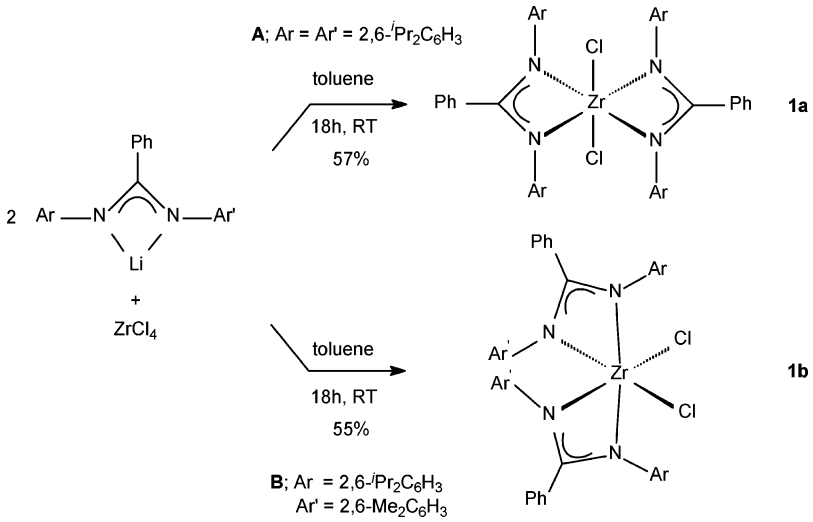

the amidinate $[p\text{-}MeC_6H_4C(NAr)_2]^-$ were reported, including a rare example of a planar four-coordinate bisamidinate magnesium compound.[9] A similar amidinate, $[PhC(NAr)_2]^-$, has been used to generate a four-coordinate high-spin Fe(II) complex with planar geometry.[10] This ligand has also been successfully applied in the synthesis of dialkyl and cationic monoalkyl derivatives of the group 3 metals and lanthanides, which are otherwise inaccessible due to ligand redistribution reactions.[11] Here we describe the synthesis and characterization of neutral dichloride, dimethyl, and cationic monomethyl bisamidinate complexes of zirconium, supported by the amidinate ligands $[PhC(NAr)_2]^-$ (**A**) and $[PhC(NAr)(NAr')]^-$ (**B**) (Ar = 2,6-^{i}Pr$_2$C$_6$H$_3$; Ar′ = 2,6-$Me_2C_6H_3$, Figure 1). X-ray crystallographic studies on complexes with the sterically most demanding amidinate **A** have established an unprecedented *trans*-Cl_2 configuration for the neutral dichloride complex, as well as tetragonal-pyramidal coordination geometry for the 10-electron cationic monoalkyl derivative.

Results and Discussion

Synthesis and Crystallographic Characterization of Dichloride Complexes. The bisamidinate dichloride complexes $[PhC(NAr)_2]_2ZrCl_2$ (**1a**) and $[PhC(NAr)(NAr')]_2ZrCl_2$ (**1b**) (Ar = 2,6-^{i}Pr$_2$C$_6$H$_3$, Ar′ = 2,6-$Me_2C_6H_3$) were prepared by the reaction of $ZrCl_4$ with 2 equiv of Li-amidinate in toluene and were obtained as orange (**1a**) or yellow (**1b**) crystals in 57 and 55% yield, respectively, by crystallization from hot hexane. X-ray crystallographic analysis of **1a** was attempted at 100 and 200 K. From the diffraction data collected at these temperatures the unit cell could not be unambiguously determined. Determination of the crystal structure at 293 K was successful in a tetragonal setting, and the problems encountered at lower temperatures may be related to a phase transition occurring upon cooling. Whereas all known group 4 metal complexes of the type (amidinate)$_2$MX$_2$ exhibit the (electronically preferred) *cis*-X_2 geometry,[5,6b,7c,12] crystallographic analysis of **1a** shows it to adopt the unusual *trans*-Cl_2 configuration. Compound **1a** crystallizes in the chiral space group $P4_32_12$ with a crystallographically imposed C_2-axis through the carbon atoms of the amidinate backbone (Figure 2, pertinent interatomic distances and angles in Table 1). The molecule is chiral due to the propeller-shaped arrangement of the aromatic substituents on the amidinate ligands, and it crystallizes without enantiomeric twinning (Flack's refinement converging at $x = -0.01(4)$).[13] The central zirconium atom is coordinated by two *N*,*N*′-dihapto amidinate ligands and two chlorides. The two amidinate ligands occupy the equatorial positions and two chlorides are axial, *trans* relative to each other (Cl(1)−Zr−Cl(1a) = 179.73(3)°). The two amidinate ligand planes (N−C−N−Zr) are only slightly tilted (11.06(12)°) with respect to each other. The planar four-coordinate geometry of Mg[9] and Fe[10] bisamidinate complexes with the same ligand type was attributed to steric effects. The crystal structure of **1b**, with sterically slightly less demanding amidinate ligands, indeed shows a normal *cis*-Cl_2 geometry (Figure 2, pertinent interatomic distances and angles in Table 1). Apparently, unfavorable steric interactions between the four 2,6-diisopropylphenyl substituents in **1a** result in the *trans*-Cl_2 geometry being the most stable. It should be noted that for the smaller Fe(II) ion the bisamidinate complex with ligand **B** still retains the planar geometry.[10]

The Zr−Cl bond distance in **1b** (2.3997(8) Å) is smaller by 0.037 Å relative to that in **1a** and is comparable to that found for other structurally characterized bisamidinate complexes of zirconium.[5,7c,12] The sterically most demanding 2,6-^{i}PrC$_6$H$_3$ substituents are found on the N atoms located *trans* to each other (N(1)−Zr−(N1a), 174.09(9)°), whereas the xylyl substituents are placed on the two *cis* nitrogen atoms (N(2)−Zr−N(2a), 88.18(9)°), occupying the more crowded equatorial

(9) Boeré, R. T.; Cole, M. L.; Junk, P. C. *New J. Chem.* **2005**, *29*, 128.

(10) Nijhuis, C. A.; Jellema, E.; Sciarone, T. J. J.; Meetsma, A.; Budzelaar, P. H. M.; Hessen, B. *Eur. J. Inorg. Chem.* **2005**, 2089.

(11) (a) Bambirra, S.; van Leusen, D.; Meetsma, A.; Hessen, B.; Teuben, J. H. *Chem. Commun.* **2003**, 522. (b) Bambirra, S.; Bouwkamp, M. W.; Meetsma, A.; Hessen, B. *J. Am. Chem. Soc.* **2004**, *126*, 9182.

(12) Roesky, H. W.; Meller, B.; Noltemeyer, M.; Schmidt, H. G.; Scholz, U.; Sheldrick, G. M. *Chem. Ber.* **1988**, *121*, 1403.

(13) (a) Flack, H. D. *Acta Crystallogr. A* **1983**, *39*, 876. (b) Flack, H. D.; Bernardinelli, G. *Acta Crystallogr. A* **1999**, *55*, 908. (c) Flack, H. D.; Bernardinelli, G. *J. Appl. Crystallogr.* **2000**, *33*, 1143. (d) Herbst-Irmer, R.; Sheldrick, G. M. *Acta Crystallogr. B* **1998**, *54*, 443.

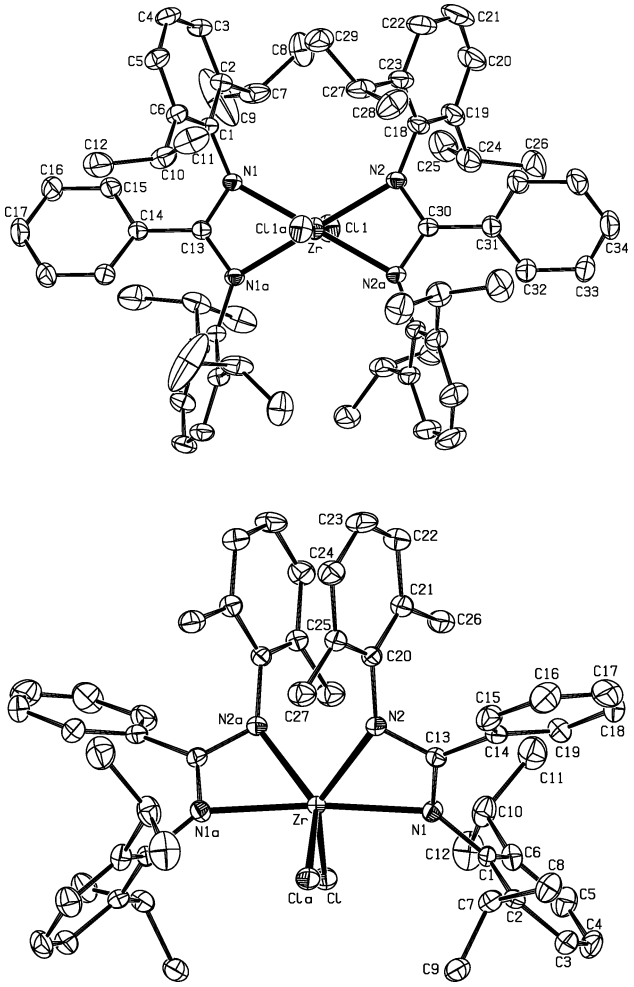

Figure 2. Molecular structure of $(\mathbf{A})_2ZrCl_2$ (**1a**, top) showing 20% probability ellipsoids and $(\mathbf{B})_2ZrCl_2$ (**1b**, bottom) showing 50% probability ellipsoids.

Table 1. Selected Bond Distances (Å) and Angles (deg) for $(\mathbf{A})_2ZrCl_2$ (1a) and $(\mathbf{B})_2ZrCl_2$ (1b)

1a		1b	
Zr−N(1)	2.217(2)	Zr−N(1)	2.309(2)
Zr−N(2)	2.207(2)	Zr−N(2)	2.180(2)
Zr−Cl(1)	2.4369(10)	Zr−Cl(1)	2.3997(8)
N(1)−C(13)	1.341(3)	N(1)−C(13)	1.322(4)
N(2)−C(30)	1.343(3)	N(2)−C(13)	1.347(4)
Cl(1)−Zr−Cl(1a)	179.73(3)	Cl(1)−Zr−Cl(1a)	105.38(3)
N(1)−Zr−N(2a)	174.44(8)	N(1)−Zr−N(1a)	174.09(9)
N(1)−Zr−N(1a)	60.29(7)	N(1)−Zr−N(2)	58.87(9)
N(2)−Zr−N(2a)	60.43(7)		
N(1)−Zr−N(2)	119.95(7)	N(2)−Zr−N(2a)	88.18(9)

positions. For **1a**, bonding of the amidinate ligands to the metal center is essentially symmetrical (bond distances N(1)−C(13) and N(2)−C(30) are identical), and for both **1a** and **1b** complete charge delocalization within the amidinate backbone is observed ($\Sigma_{\angle N}$ = 357−360°).

The *trans*-Cl_2 configuration for **1a** is unprecedented for group 4 metal L_2MX_2 complexes with two bidentate ligands. Indeed, for Fujita's zirconium complexes supported by phenoxy-imine ligands, DFT calculations indicate the *cis* to be favored over the *trans* geometry by ca. 33 kJ·mol^{-1}.[14] Six-coordinate titanium complexes with planar tetradentate salen-type[15] or porphyrin ligands[16] with *trans* geometry have been reported. Heavier group 4 elements, due to their larger ionic size, form *cis* complexes with these ligands.[17] Recently, Brintzinger and co-workers reported zirconium complexes with bianiline-based N_4-donor ligands of the type N_4ZrX_2 that have the four N atoms approximately in one plane, with the X ligands occupying axial-like positions (X−Zr−X angles of 134.5−138.4°).[18]

Synthesis and Crystallographic Characterization of Dimethyl Complexes. Synthesis of alkyl species starting from bisamidinate group 4 metal chlorides is generally achieved by reaction of the dichloride precursors with alkyllithium or Grignard reagents.[5b−d,6b,7c] Treatment of the dichlorides **1a** and **1b** with 2 equiv of MeLi in Et_2O at ambient temperature gave the dimethyl complexes **2a** and **2b** as air-sensitive crystalline material in 63 and 65% isolated yields, respectively (Scheme 2).

Compounds **2a** and **2b** were characterized by single-crystal X-ray diffraction, and the molecular structures are shown in Figure 3, with pertinent interatomic distances and angles in Table 2. The quality of the data set for **2a** is rather poor, with only about half of the unique, merged reflections obeying the $F_o \geq 4\sigma(F_o)$ criterion of observability. Two large residual peaks of 6.78 and 6.27 e/Å^3 at chemically nonrelevant positions (nearest non-hydrogen atoms: isopropyl Me C(231) at 1.50 Å and Ar *p*−C C(254) at 2.28 Å, respectively) result from the final difference Fourier synthesis, possibly due to twinning that could not be satisfactorily modeled. Nevertheless, the connectivity for the non-hydrogen atoms is unambiguously established. Surprisingly, X-ray crystallographic analysis of both **2a** and **2b** reveals complexes with *cis*-Me_2 geometry, in marked contrast to the *trans*-dichloride **1a**. Two independent molecules of **2a** are located within the unit cell, with comparable bond distances and angles, and only one is discussed. Zr−Me bond distances for **2a** (2.243(6) and 2.247(7) Å) are similar to the values reported for other bisamidinate complexes of zirconium (∼2.24 Å),[5b,d,6b,7c] whereas the Zr−Me bond in **2b** is somewhat shorter at 2.226(5) Å. For both complexes all nitrogen atoms are planar ($\Sigma_{\angle N}$ = 359.9−360.0°), indicative of complete charge delocalization. The crowding in **2a** due to the diisopropylphenyl groups in equatorial position is reflected by the relatively acute *trans* N−Zr−N angle (170.66(17) vs 173.31(11)° in **2b**), bent toward the Zr−Me cleft, and a concomitant increase in the *cis* N−Zr−N angle (94.14(18)° vs 87.93(12)°).

NMR Characterization and Solution Dynamics. Solution structures and fluxional behavior for the dichloride complexes **1a** and **1b** and the dimethyl analogues **2a** and **2b** were studied by NMR spectroscopy. In the room temperature ^{1}H NMR spectrum of **1a**,

(14) Matsui, S.; Mitani, M.; Saito, J.; Tohi, Y.; Makio, H.; Matsukawa, N.; Takagi, Y.; Tsuru, K.; Nitabaru, M.; Nakano, T.; Tanaka, H.; Kashiwa, N.; Fujita, T. *J. Am. Chem. Soc.* **2001**, *123*, 6847.

(15) (a) Mazzanti, M.; Rosset, J. M.; Floriani, C.; Chiesivilla, A.; Guastini, C. *J. Chem. Soc., Dalton Trans.* **1989**, 953. (b) Floriani, C.; Solari, E.; Corazza, F.; Chiesivilla, A.; Guastini, C. *Angew. Chem., Int. Ed. Engl.* **1989**, *28*, 64.

(16) (a) Lecomte, C.; Protas, J.; Marchon, J. C.; Nakajima, M. *Acta Crystallogr. B* **1978**, *34*, 2856. (b) Marchon, J. C.; Latour, J. M.; Grand, A.; Belakhovsky, M.; Loos, M.; Goulon, J. *Inorg. Chem.* **1990**, *29*, 57.

(17) (a) Corazza, F.; Solari, E.; Floriani, C.; Chiesivilla, A.; Guastini, C. *J. Chem. Soc., Dalton Trans.* **1990**, 1335. (b) Black, D. G.; Swenson, D. C.; Jordan, R. F.; Rogers, R. D. *Organometallics* **1995**, *14*, 3539.

(18) Kettunen, M.; Vedder, C.; Schaper, F.; Leskelä, M.; Mutikainen, I.; Brintzinger, H. H. *Organometallics* **2004**, *23*, 3800.

Scheme 2

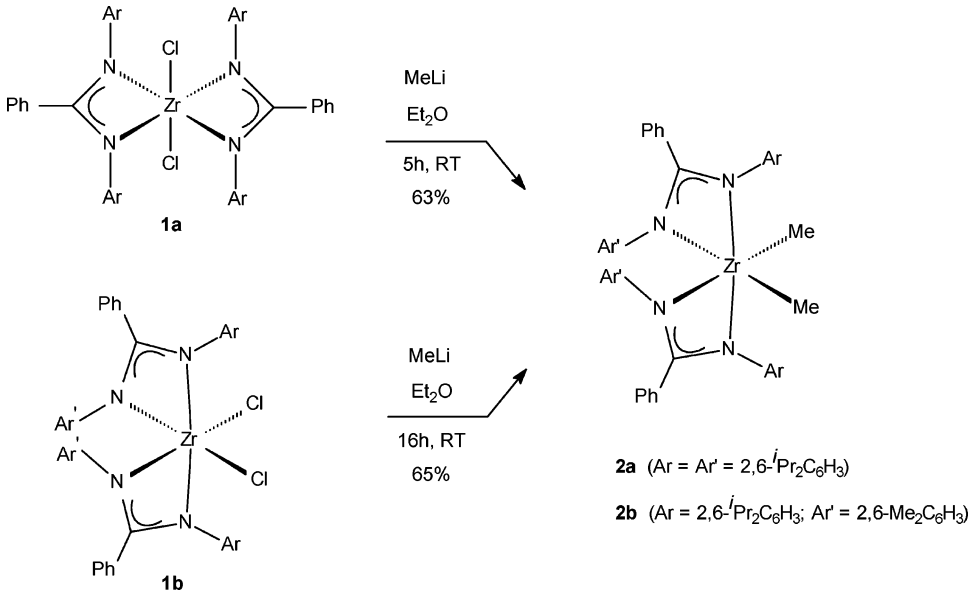

two inequivalent isopropyl groups are observed, with CH resonances at δ 4.01 and 3.38 ppm and diastereotopic Me groups at δ 1.49, 1.47, 0.83, and 0.12 ppm. The solution NMR spectrum is thus consistent with the solid state structure, in which the helical "propeller" arrangement of the aromatic substituents renders the complex chiral. Interconversion of the two enantiomers can be achieved by a concerted flip of the screw sense of the arrangement of the aromatic rings via a D_{2h} symmetric transition state (Scheme 3).[10]

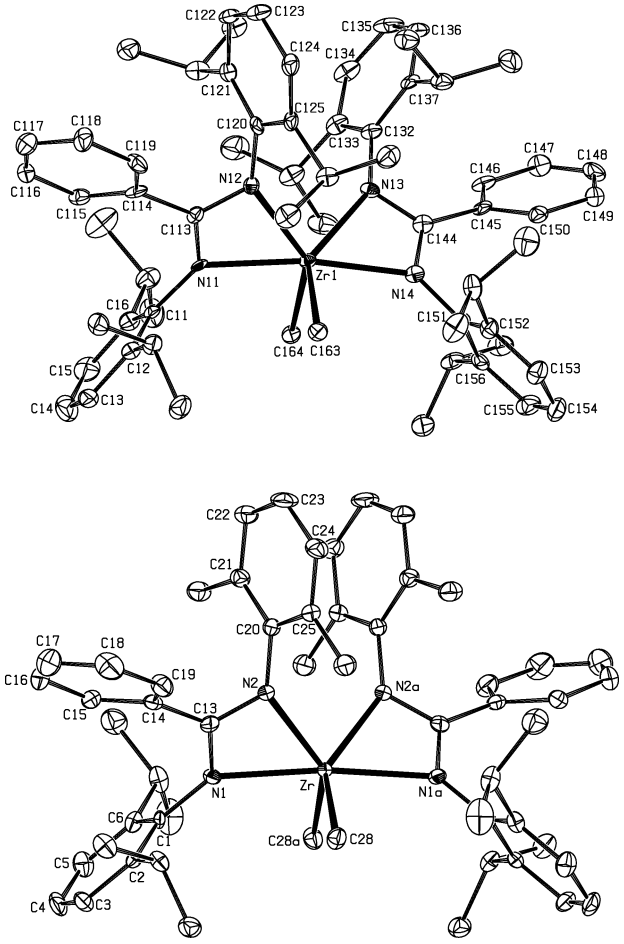

Figure 3. Molecular structure of $(\mathbf{A})_2ZrMe_2$ (**2a**, top) and $(\mathbf{B})_2ZrMe_2$ (**2b**, bottom) showing 50% probability ellipsoids. Labels of the isopropyl and xylyl methyl groups are omitted for clarity.

Table 2. Selected Bond Distances (Å) and Angles (deg) for $(A)_2ZrMe_2$ (2a) and $(B)_2ZrMe_2$ (2b)

2a		2b	
Zr(1)−C(163)	2.243(6)	Zr−C(28)	2.226(5)
Zr(1)−C(164)	2.247(7)		
Zr(1)−N(11)	2.337(5)	Zr−N(1)	2.341(3)
Zr(1)−N(12)	2.263(5)	Zr−N(2)	2.224(3)
Zr(1)−N(13)	2.280(4)		
Zr(1)−N(14)	2.318(5)		
N(11)−C(113)	1.327(8)	N(1)−C(13)	1.331(5)
N(12)−C(113)	1.358(7)	N(2)−C(13)	1.338(5)
N(13)−C(144)	1.353(7)		
N(14)−C(144)	1.341(8)		
C(163)−Zr(1)−C(164)	93.7(2)	C(28)−Zr−C(28a)	100.71(16)
N(13)−Zr(1)−C(163)	137.00(18)	N(2a)−Zr−C(28)	136.62(15)
N(12)−Zr(1)−C(164)	136.89(18)		
N(11)−Zr(1)−N(14)	170.66(17)	N(1)−Zr−N(1a)	173.31(11)
N(12)−Zr(1)−N(13)	94.14(18)	N(2)−Zr−N(2a)	87.93(12)
N(11)−Zr(1)−N(13)	129.74(15)	N(1)−Zr−N(2a)	127.91(11)
N(12)−Zr(1)−N(14)	130.42(17)		

Warming a toluene-d_8 solution of **1a** in a 200 MHz NMR spectrometer reveals fluxional behavior in which the two isopropyl CH resonances coalesce at 91.8 ± 0.5 °C into a single broad line. This may be due to the interconversion of the molecular helicity through a D_{2h} symmetric transition state (Scheme 3), and a barrier of $\Delta G_{Tc}^{\ddagger} = 72.9 \pm 0.2$ kJ·mol^{-1} was determined for this process.[19] Cooling the sample to −60 °C does not result in any change relative to the room-temperature spectrum. Variable-temperature 2D EXSY measurements were performed in order to determine the enthalpic and entropic contribution to the overall activation barrier (see Supporting Information for details).[20] Spectra were recorded at 14.5, 24.4, 34.3, 44.2, and 53.9 °C, and at each temperature, four mixing times were chosen such

(19) Hesse, M.; Meier, H.; Zeeh, B. *Spectroscopic Methods in Organic Chemistry*; Georg Thieme Verlag: Stuttgart, New York, 1997; pp 95−100.

(20) (a) Abel, E. W.; Coston, T. P. J.; Orrell, K. G.; Šik, V.; Stephenson, D. *J. Magn. Reson.* **1986**, *70*, 34. (b) Perrin, C. L.; Dwyer, T. J. *Chem. Rev.* **1990**, *90*, 935.

Scheme 3[a]

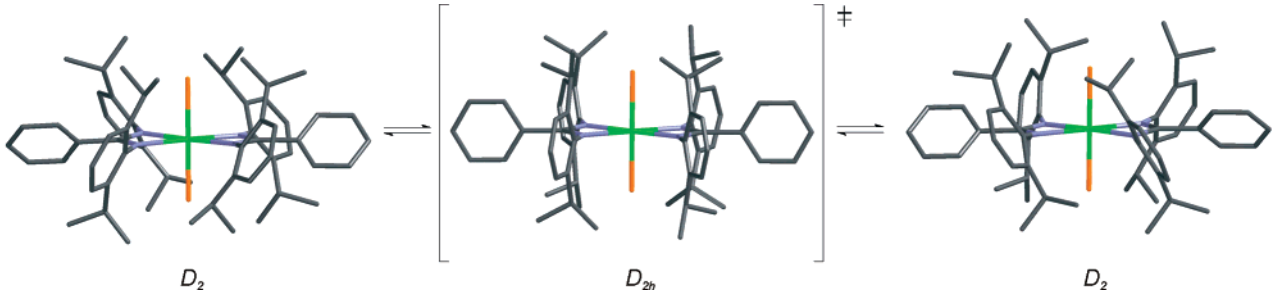

[a] Graphics are generated using Spartan.[43] These do not represent ground or transition states from calculations, but serve as a guide to the eye only.

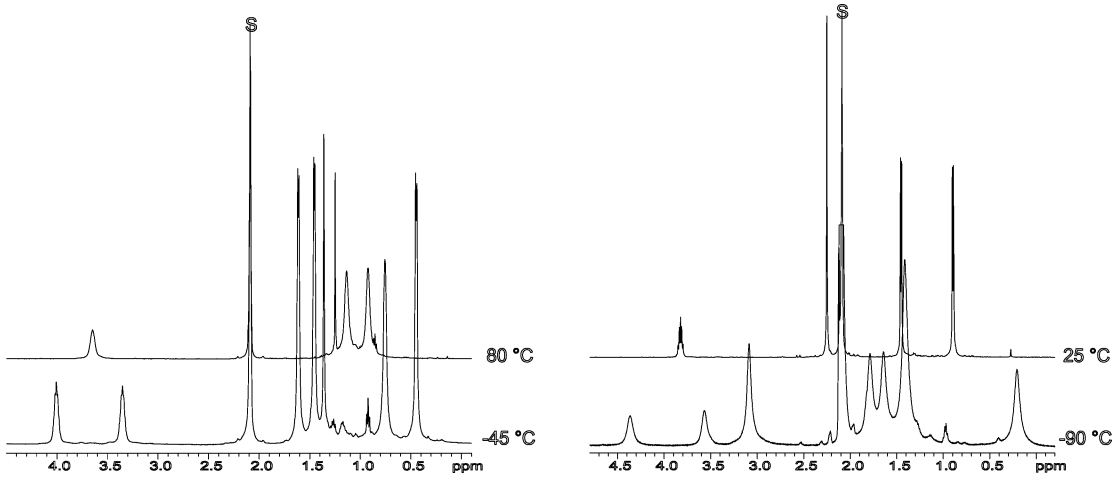

Figure 4. Variable-temperature ^{1}H NMR spectra of **2a** (left) and **1b** (right, 500 MHz, toluene-d_8 solvent, S denotes residual solvent resonance).

that cross-peak intensities varied sufficiently to allow for extraction of the activation parameters. Volumes of the isopropyl CH diagonal- and cross-peaks in the 2D spectra were obtained by the Gaussian fit integration method implemented in Sparky.[21] Fitting the data gave $\Delta H^{\ddagger} = 72.5 \pm 1.8$ kJ·mol^{-1} and $\Delta S^{\ddagger} = -6.8 \pm 5.9$ J·mol^{-1}·K^{-1}. The entropy of activation is small and slightly negative, which seems to rule out a dissociative mechanism. Instead, the data support a rearrangement from a ground state with relatively few degrees of freedom, through a six-coordinate transition state. Extrapolation leads to $\Delta G^{\ddagger} = 75.1 \pm 4.0$ kJ·mol^{-1} at 91.8 °C, which compares reasonably well to the value (72.9 $\pm$ 0.2 kJ·mol^{-1}) obtained by the 1D coalescence method. At room temperature, the rate constant for racemization is calculated to be 0.5 s^{-1}, and thus conversion of one enantiomer to the racemic mixture proceeds with a half-life time of about 0.7 s. Consistent with this, solutions, prepared by dissolving one large (~2−3 mg) single crystal of **1a** in either hexane or dichloromethane at ambient temperature, displayed no optical rotation (measurement taken ca. 5 min after dissolution).

The ^{1}H NMR spectrum of the dimethyl compound **2a** at −90 °C is broad, but consistent with the solid state C_2 symmetric *cis*-Me_2 structure, showing the presence of four inequivalent isopropyl groups. Thus, while other group 4 metal bisamidinate complexes reported in the literature show NMR characteristics evidencing rapid ligand rearrangement,[5b,7c,12] **2a** offers a unique opportunity to study the kinetics of rearrangements in these C_2 symmetric bisamidinate compounds.[22] For the titanium bisguanidinate complex $[Me_2NC(N^iPr)_2]_2TiCl_2$ NMR spectra also indicate C_2 symmetry at low temperature, but no kinetic data on the fluxional process have been reported.[23] Around −84 °C the isopropyl CH resonances coalesce, and above that temperature two isopropyl groups are observed. The remaining isopropyl CH resonances coalesce at 22.5 °C, and further warming the sample to 80 °C results in sharp NMR lines (δ 3.65 (^{i}Pr CH), 1.14, 0.92 (^{i}Pr Me), and 1.25 ppm (Zr−Me)) (Figure 4). For the two dynamic processes observed in **2a**, the free energy of activation $\Delta G_{Tc}^{\ddagger}$ is found to be 56.2 $\pm$ 0.2 kJ·mol^{-1} for the process with $T_c = 22.5 \pm 0.5$ °C. The low-temperature process with $T_c = -84 \pm 2$ °C requires an estimated activation energy $\Delta G_{Tc}^{\ddagger}$ of about 35 kJ·mol^{-1}, but in this case the slow exchange limit could not be fully reached.

Similar variable-temperature NMR characteristics are observed for **1b**. At −90 °C, the ^{1}H NMR spectrum in toluene-d_8 features two sets of resonances for both the isopropyl and xylyl Me groups (Figure 4). Warming the solution results in coalescence, with $T_c = -70 \pm 1$ °C for the isopropyl CH signals, corresponding to $\Delta G_{Tc}^{\ddagger} = 37.6 \pm 0.3$ kJ·mol^{-1}. At room temperature, one isopropyl group (δ 3.83 (^{i}Pr CH), 1.45 and 0.90 ppm

(21) Goddard, T. D.; Kneller, D. G. *SPARKY 3*; University of California: San Francisco.

(22) For $[^tBuC(NCy)_2]_2ZrCl_2$, inequivalent cyclohexyl groups were observed in the low-temperature ^{13}C NMR spectrum.[5d] Fluxional behavior in $[PhC(NSiMe_3)_2]_2ZrX_2$ complexes with X = benzyl or allyl[5b] or ZrX_2 = metalacycle[7c] has been described.

(23) Mullins, S. M.; Duncan, A. P.; Bergman, R. G.; Arnold, J. *Inorg. Chem.* **2001**, *40*, 6952.

Scheme 4

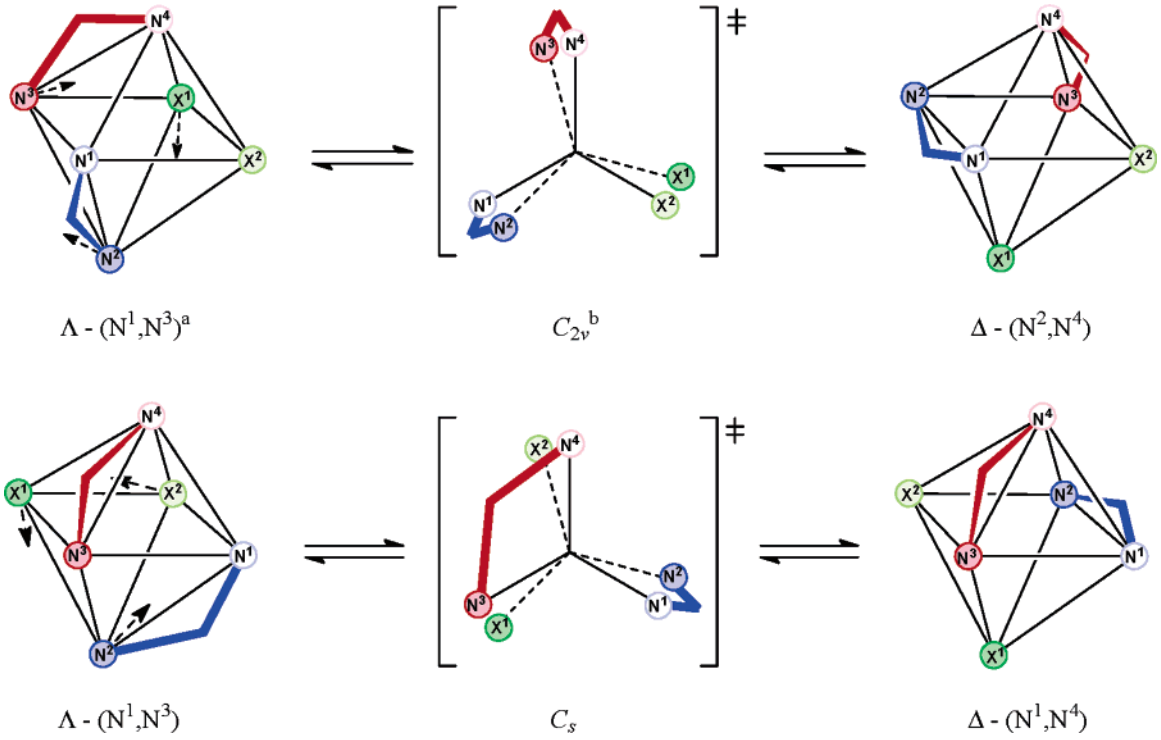

[a] Indicated in brackets are the nitrogen atoms found in the same plane as the X ligands. [b] The C_{2v} symmetric transition state with amidinate ligands spanning triangular faces is sterically disfavored.

(*i*Pr Me)) as well as one xylyl Me resonance (δ 2.25 ppm) is observed. For complex **2b**, the ^{1}H NMR spectrum at room temperature is sharp, featuring one set of signals for the isopropyl groups as well as one xylyl-Me resonance, with no sign of broadening down to −60 °C. It seems that ligand rearrangement is more facile in the dimethyl complex **2b** than for the corresponding dichloride **1b**, which is in line with X-ray crystallographic results, indicating Zr−N bond lengths in **2b** to be somewhat longer (by ∼0.04 Å).

Mechanistic insight into the dynamics in these complexes was obtained from 2D EXSY NMR experiments on **2a**. Analysis of EXSY spectra taken at −52.2, −41.9, −31.7, and −21.6 °C (where two distinct isopropyl CH resonances are observed) allows us to determine the activation parameters for the exchange process that renders all isopropyl CH groups equivalent. The values obtained are $\Delta H^{\ddagger} = 47.8 \pm 1.0$ kJ·mol^{-1} and $\Delta S^{\ddagger} = -32.8 \pm 4.1$ J·mol^{-1}·K^{-1} (see Supporting Information for details), which extrapolates to $\Delta G^{\ddagger} = 57.5 \pm 2.2$ at 22.5 °C, in excellent agreement with the activation free energy obtained from coalescence in the 1D NMR spectrum (56.2 ± 0.2 kJ·mol^{-1}). Exchange phenomena in related six-coordinate bis(chelate) complexes may occur either through a trigonal twist with retention of the six-coordinate geometry[24] or by metal−N bond rupture (dissociative mechanism) involving a transient five-coordinate intermediate.[25] From the negative entropy of activation, it is concluded that the dynamics observed for **2a** involve a twist instead of a dissociative mechanism. Consequently, it seems reasonable to assume that also the low-temperature dynamic process ($\Delta G^{\ddagger} \approx 35$ kJ·mol^{-1} at −84 °C) occurs by an internal twist mechanism. A full rotation around the amidinate−metal axis, as proposed for the dynamic process in the bisguanidinate complex $[Me_2NC(N^iPr)_2]_2TiCl_2$,[23] is likely to be precluded by the steric demand of the ligand.

Trigonal twist mechanisms for complexes of the type $(AA)_2MX_2$ or $(AB)_2MX_2$ have been studied extensively in the past,[26] both theoretically[27] and experimentally.[28] For $(AA)_2MX_2$, a single twist results in transition states with either C_{2v} or C_s symmetry (Scheme 4). The former leads to exchange of axial and equatorial sites in **2a**, while retaining the diastereotopic relationship between the two isopropyl groups on an individual diisopropylphenyl moiety, as required for the rearrangement with the lowest activation barrier. For the second dynamic process ($T_c = 22.5$ °C), the possibility to arrive at a *trans* geometry by two successive trigonal twists[28a] (through C_2 symmetric transition states, see Supporting Information) presents a possible explanation for the apparent equivalence of all isopropyl groups in the ^{1}H NMR spectrum of **2a** above room temperature. However, the activation parameters for the exchange process that results in equivalence of all isopropyl groups in the molecule are distinctly different for (*cis*-)**2a** and (*trans*-

(24) (a) Rahim, M.; Taylor, N. J.; Xin, S. X.; Collins, S. *Organometallics* **1998**, *17*, 1315. (b) Kakaliou, L.; Scanlon, W. J.; Qian, B. X.; Baek, S. W.; Smith, M. R.; Motry, D. H. *Inorg. Chem.* **1999**, *38*, 5964.
(25) (a) Gau, H. M.; Fay, R. C. *Inorg. Chem.* **1990**, *29*, 4974. (b) Bei, X. H.; Swenson, D. C.; Jordan, R. F. *Organometallics* **1997**, *16*, 3282. (c) Tsukahara, T.; Swenson, D. C.; Jordan, R. F. *Organometallics* **1997**, *16*, 3303. (d) Crust, E. J.; Clarke, A. J.; Deeth, R. J.; Morton, C.; Scott, P. *Dalton Trans.* **2004**, 4050.
(26) Serpone, N.; Bickley, D. G. *Prog. Inorg. Chem.* **1972**, *17*, 391.
(27) (a) Bickley, D. G.; Serpone, N. *Inorg. Chem.* **1976**, *15*, 948. (b) Bickley, D. G.; Serpone, N. *Inorg. Chem.* **1976**, *15*, 2577. (c) Willem, R.; Gielen, M.; Pepermans, H.; Brocas, J.; Fastenakel, D.; Finocchiaro, P. *J. Am. Chem. Soc.* **1985**, *107*, 1146.
(28) (a) Serpone, N.; Fay, R. C. *Inorg. Chem.* **1967**, *6*, 1835. (b) Bickley, D. G.; Serpone, N. *Inorg. Chim. Acta* **1978**, *28*, 169. (c) Bickley, D. G.; Serpone, N. *Inorg. Chim. Acta* **1980**, *43*, 185. (d) Willem, R.; Gielen, M.; Pepermans, H.; Hallenga, K.; Recca, A.; Finocchiaro, P. *J. Am. Chem. Soc.* **1985**, *107*, 1153. (e) Fay, R. C.; Lindmark, A. F. *J. Am. Chem. Soc.* **1983**, *105*, 2118.

Scheme 5

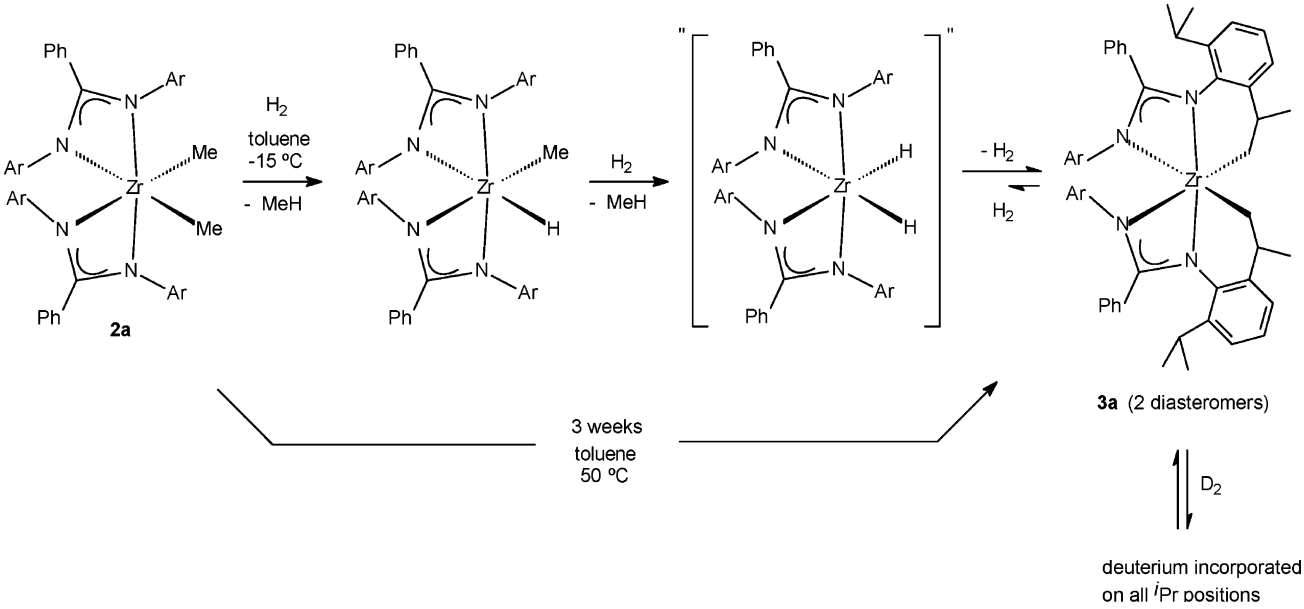

)**1a** ($\Delta H^{\ddagger} = 47.8 \pm 1.0$ vs 72.5 ± 1.8 kJ·mol^{-1} and $\Delta S^{\ddagger} = -32.8 \pm 4.1$ vs -6.8 ± 5.9 J·mol^{-1}·K^{-1}, respectively). This seems to rule out that *trans* intermediates are involved in the rearrangement of **2a**. Instead, a combination of two trigonal twists with C_s symmetric transition states can account for the NMR characteristics observed for **2a**.[28a] Comparison of the activation free energy for the two distinct exchange processes in **2a** calculated at −84 °C (35 and 54 kJ·mol^{-1} for the low- and high-temperature process, respectively) reflects the differences between the proposed transition states. As expected from steric considerations, transition states with an amidinate ligand spanning a triangular face of the trigonal prism (C_s) are higher in energy compared to those with the bidentate ligands on square faces (C_{2v}). Ligand rearrangements in the related complexes **1b** and **2b** most likely occur by a similar trigonal twist mechanism. The reduced steric requirements of the amidinate ligand in these complexes, however, significantly facilitate the dynamic processes described above.

Hydrogenolysis and Thermolysis. Reaction of the dimethyl complex **2a** with H_2 (approximately 4 bar) at ambient temperature on NMR tube scale in C_6D_6 proceeds smoothly as indicated by the rapid formation of methane. A singlet ^{1}H NMR resonance at δ 12.95 ppm is observed, which can tentatively be attributed to a monomeric, terminal group 4 metal hydride.[29] Monitoring the reaction by ^{1}H NMR spectroscopy shows the appearance of a second hydride species (singlet at δ 12.33 ppm) within 1 h, while after ca. 3 h the formation can be seen of the doubly cyclometalated complex {PhC(NAr)[NC$_6$H$_3$(^{i}Pr)(CHMeCH$_2$)]}$_2$Zr (**3a**, identified by independent synthesis, vide infra). Careful low-temperature hydrogenolysis (−15 °C, 24 h) results in a mixture of ca. 40% unreacted **2a** and 60% of the initial hydride species (Zr−H: δ 12.85 ppm at −20 °C). ^{1}H and ^{13}C NMR spectra of this mixture taken at −20 °C indicate that this initial hydride species is (**A**)$_2$Zr(H)(Me), with Zr−Me resonances at δ 1.22 (^{1}H) and 63.90 ppm (^{13}C) (for **2a**: δ 1.33 and 57.76 ppm). After 3 days at −15 °C this species had given way to the second hydride (Zr−H: δ 12.28 ppm). The slow concomitant appearance of the metalated complex **3a** makes it more difficult to deduce the nature of this species from NMR data. Nevertheless, the absence of new Zr−C resonances in the ^{13}C NMR spectrum seems to suggest that it is (**A**)$_2$ZrH$_2$ (Scheme 5). Performing the reaction of **2a** with D_2 in C_6H_6 in an NMR tube at ambient temperature results in the formation of methane-d_1 and zirconium deuteride complexes (δ 12.93 and 12.31 ppm in the ^{2}H NMR spectrum), which also react further to form **3a**. Evidence for the reverse reaction (hydrogenolysis/deuterogenolysis of the cyclometalated Zr−CH$_2$ bond) comes from the observation that deuterium is slowly incorporated on both the isopropyl methyl and methine groups when **3a** is reacted with D_2, with concomitant formation of HD and H_2. Similar observations have been made, for example, for a triamidoamine monobenzyl zirconium complex reported by Scott.[30] Although d^0 metal hydrides tend to dimerize or oligomerize,[29b] the present results indicate that monomeric hydride species are accessible when sterically demanding amidinate ligands are employed. Unfortunately, in our system the subsequent reactivity with the isopropyl groups on the ligand system precludes isolation and full characterization of such monomeric hydrides.

Warming an NMR sample of **2a** (toluene-d_8 solution) at 50 °C in the dark for 3 weeks also leads to formation of **3a** as a mixture of diastereomers, with liberation of methane (Scheme 5). Recently, Eisen and co-workers reported trimethylsilyl CH bond activation for the bisamidinate complex [p-MeC$_6$H$_4$C(NSiMe$_3$)$_2$]$_2$TiMe$_2$ to give [p-MeC$_6$H$_4$C-(NSiMe$_3$)(NSiMe$_2$CH$_2$)]$_2$Ti, which was found cocrystallized (22%) with the dimethyl precursor.[6b]

Crystals suitable for X-ray analysis were obtained by diffusion of pentane into a C_6D_6 solution of **3a**. After solving the structure by Patterson methods, a difference Fourier synthesis revealed that some atoms partially occupied two positions, corresponding to two different

(29) (a) Chirik, P. J.; Day, M. W.; Bercaw, J. E. *Organometallics* **1999**, *18*, 1873. (b) Hoskin, A. J.; Stephan, D. W. *Coord. Chem. Rev.* **2002**, *233*, 107.

(30) Morton, C.; Munslow, I. J.; Sanders, C. J.; Alcock, N. W.; Scott, P. *Organometallics* **1999**, *18*, 4608.

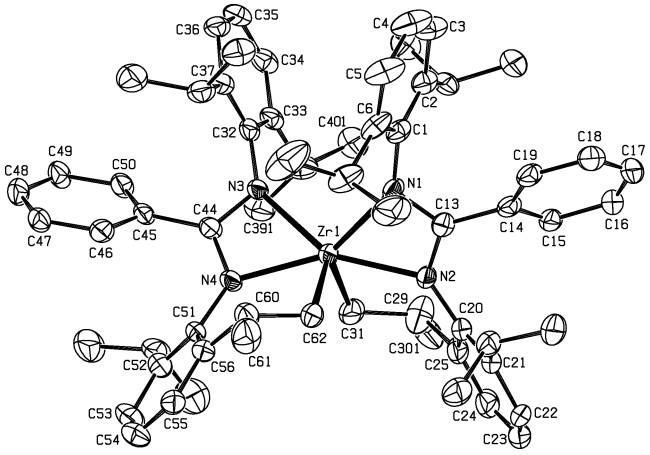

Figure 5. Molecular structure of {PhC(NAr)[NC_6H_3(*i*Pr)-($CHMeCH_2$)]}$_2$Zr (**3a**, major fraction) showing 50% probability ellipsoids. Labels of the isopropyl groups are omitted for clarity.

Table 3. Selected Bond Distances (Å) and Angles (deg) for {PhC(NAr)[NC_6H_3(*i*Pr)($CHMeCH_2$)]}$_2$Zr (3a)

Zr(1)−C(31)	2.258(4)	C(31)−Zr(1)−C(62)	108.63(15)
Zr(1)−C(62)	2.241(4)	N(1)−Zr(1)−C(31)	126.59(12)
Zr(1)−N(1)	2.292(3)	N(3)−Zr(1)−C(62)	125.85(13)
Zr(1)−N(2)	2.207(3)	N(1)−Zr(1)−N(2)	58.78(11)
Zr(1)−N(3)	2.299(3)	N(3)−Zr(1)−N(4)	58.67(11)
Zr(1)−N(4)	2.209(3)	N(2)−Zr(1)−N(4)	151.47(11)
N(1)−C(13)	1.352(5)	N(1)−Zr(1)−N(3)	101.83(11)
N(2)−C(13)	1.327(5)	N(2)−Zr(1)−N(3)	147.72(11)
N(3)−C(44)	1.351(4)	N(1)−Zr(1)−N(4)	143.93(10)
N(4)−C(44)	1.327(5)		

diastereomers that are cocrystallized (vide infra). Figure 5 shows the molecular structure of **3a** with C(30), C(39), and C(40) represented by the major fraction present in the crystal; pertinent bond distances and angles are listed in Table 3.

The X-ray diffraction study of **3a** corroborates the presence of two cyclometalated amidinate ligands. The central zirconium atom is surrounded in a highly distorted octahedral environment by four nitrogen atoms and two methylene carbons bridging to the ligand. A notable metrical difference between the dimethyl complex **2a** and the cyclometalated complex **3a** is the N(2)−Zr(1)−N(4) angle of 151.47(11)°, which is substantially smaller than the 170.66(17)° found for **2a**, emphasizing the strain that accompanies the formation of the six-membered metalacycle. Consequently, Zr(1)−N(2) and Zr(1)−N(4) distances (2.207(3) and 2.209(3) Å) are relatively short compared to those in **2a** (2.337(5) and 2.318(5) Å). The other Zr−N distances are somewhat longer (by ∼0.06 Å) and the CH_2−Zr−CH_2 angle is larger (108.64(15)°) than the Me−Zr−Me angle in the dimethyl complex **2a** (93.7(2)°).

NMR spectroscopic analysis of **3a** (^{1}H, ^{13}C, COSY, and HSQC) is fully consistent with the structure as observed in the single-crystal structure determination. The ^{1}H NMR spectrum of **3a** shows three sets of signals that can be attributed to two distinct products: a C_2 symmetric complex (*S*,*S* diastereomer) giving rise to one set and a C_1 symmetric (*S*,*R*) compound with two sets of resonances for the metalated $CHMeCH_2$Zr fragment. A second possible C_2 symmetric complex (*R*,*R* diastereomer) was observed as a minor reaction product (<5%), reflecting the unfavorable sterics for that configuration. Furthermore, the observed coupling constants $^3J_{HH}$ in the $CHMeCH_2$Zr fragment are in excellent agreement with the values predicted on the basis of the dihedral angles from the X-ray structure.[31] In the ^{13}C NMR spectrum, three triplets characteristic of the CH_2Zr groups are observed at δ 85.40 and 83.89 ppm for the C_1 and δ 84.85 ppm for the C_2 symmetric complex. The coupling constant $^1J_{CH}$ for these triplets (116 Hz) is similar to that for the Zr−Me groups in **2a**. After full conversion (ca. 3 weeks), a 2:1 mixture of the two isomers is obtained (in favor of the *S*,*R* diastereomer), which could not be separated by crystallization. Monitoring the thermolysis by ^{1}H NMR confirms the C_1 symmetric complex (*S*,*R*) to be the initial (kinetic) product, whereas prolonged heating slowly converts the mixture into the thermodynamically most stable C_2 symmetric product (*S*,*R*:*S*,*S* ≈ 1:2 after 6 weeks at 50 °C). This observation is consistent with the predominant formation of the kinetic cyclometalation product after room-temperature hydrogenolysis of **2a** (*S*,*R*:*S*,*S* ≈ 4:1).

Synthesis, Characterization, and Reactivity of Cationic Zr−Methyl Derivatives. Reaction of **2a** with a stoichiometric amount of $B(C_6F_5)_3$ or [$PhNMe_2H$]-[$B(C_6F_5)_4$] in C_6D_5Br at room temperature quantitatively gives the ionic species [(**A**)$_2$ZrMe][$RB(C_6F_5)_3$] (R = Me, **4a**; R = C_6F_5, **5a**; Scheme 6). Removal of C_6D_5Br from a solution of **5a** under reduced pressure and subsequent addition of toluene gave a yellow-greenish oil, which solidified in the course of 2 days to give X-ray quality crystals. A single-crystal structure determination encountered a disorder problem in that the cation appears to be present in the lattice in two different orientations, in which the Zr−Me moiety is located either above or below the N_4 plane. This could be described by a two-site occupancy model, for which the two fractions were separately refined (the sof for the minor fraction refining to 0.26). Due to the essentially planar arrangement of the two amidinate ligands that dominate the crystal packing, this disorder has little effect on the ligand geometry. The structure determination revealed that the cationic moiety adopts a distorted tetragonal-pyramidal conformation with the Me group occupying the apical position (Figure 6, pertinent interatomic distances and angles in Table 4). The nitrogen atoms of the two amidinate ligands form a slightly twisted (16.2(2)°) base for the pyramidal structure, with the central Zr atom located 0.801(2) Å out of this plane. The Zr−Me distance in **5a** is only marginally shorter than those in **2a**, whereas the Zr−N bond lengths in **5a** are on average 0.054 Å shorter.

The tetragonal-pyramidal conformation observed for **5a** resembles the *trans*-Cl_2 geometry of **1a**, with one axial ligand lacking. This is supported by solution ^{1}H and ^{13}C NMR spectroscopy. ^{1}H NMR resonances of the cationic moieties of **4a** and **5a** are identical, with isopropyl signals at δ 3.00, 2.65 (2×), and 2.46 ppm (CH) and eight doublets between δ 1.43 and −0.04 ppm (Me). The Zr−Me signal is observed at δ 1.72 (^{1}H) and 68.77 ppm (^{13}C), both downfield from the neutral dimethyl complex **2a** (δ 1.28 and 57.51 ppm). ^{19}F NMR spectra for the [$MeB(C_6F_5)_3$] anion in **4a** are indicative of a solvent-separated ion pair (Δδ(*p*,*m*-F) = 2.43).[32] At room

(31) Hesse, M.; Meier, H.; Zeeh, B. *Spectroscopic Methods in Organic Chemistry*; Georg Thieme Verlag: Stuttgart, New York, 1997; pp 108−109.

Scheme 6

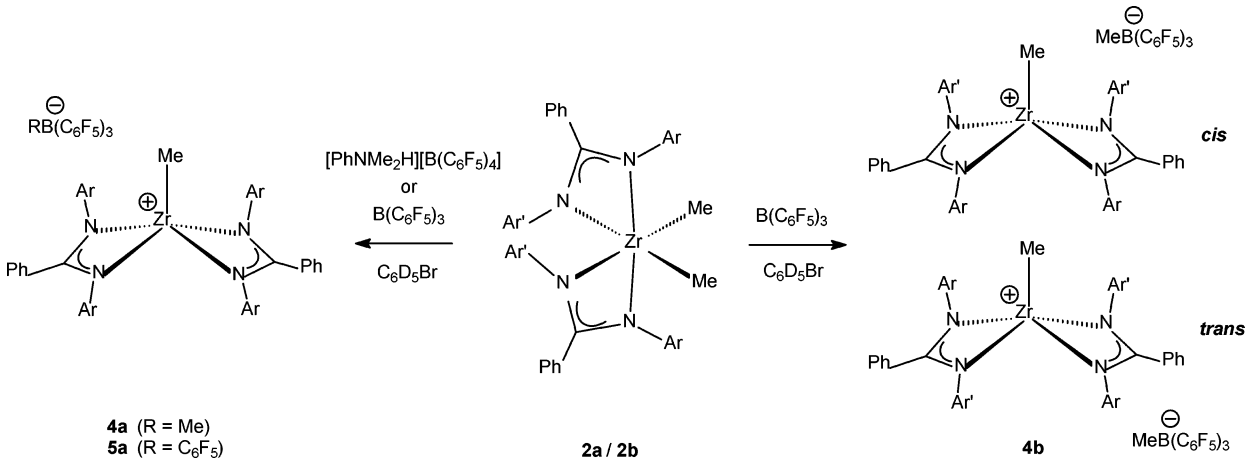

Table 4. Selected Bond Distances (Å) and Angles (deg) for [(A)$_2$ZrMe][B(C$_6$F$_5$)$_4$] (5a)

Zr(111)−C(163)	2.236(6)	N(11)−Zr(111)−N(12)	61.40(15)
Zr(111)−N(11)	2.187(4)	N(13)−Zr(111)−N(14)	59.87(16)
Zr(111)−N(12)	2.163(4)	N(11)−Zr(111)−N(13)	128.79(16)
Zr(111)−N(13)	2.244(4)	N(12)−Zr(111)−N(14)	145.67(16)
Zr(111)−N(14)	2.196(4)	N(11)−Zr(111)−C(163)	116.38(18)
N(11)−C(113)	1.338(6)	N(12)−Zr(111)−C(163)	108.98(19)
N(12)−C(113)	1.354(6)	N(13)−Zr(11)−C(163)	114.78(19)
N(13)−C(144)	1.343(6)	N(14)−Zr(11)−C(163)	105.33(19)
N(14)−C(144)	1.354(6)		

temperature, the ^{1}H NMR spectrum is static, with four inequivalent isopropyl groups: in analogy to **1a**, flipping of the "propeller blades" (inversion of helicity) is slow on the NMR time scale. 2D EXSY experiments (at 24.4, 44.2, 63.5, and 82.3 °C) on C_6D_5Br solutions of **5a** show exchange in pairs between the four different isopropyl groups. Integration of 2D diagonal- and cross-peaks (^{i}Pr Me resonances at δ 1.43 and −0.04 ppm) and numerical analysis gave $\Delta H^{\ddagger} = 77.6 \pm 1.1$ kJ·mol^{-1} and $\Delta S^{\ddagger} = 0.5 \pm 3.3$ J·mol^{-1}·K^{-1} (see Supporting Information for details). The activation enthalpy is somewhat higher than for the neutral dichloride complex **1a**, consistent with the shortened Zr−N bond lengths in **5a** leading to a stronger steric interaction between the amidinate substituents.

Reaction of **2b** with $B(C_6F_5)_3$ in C_6D_5Br results in clean methide abstraction to give the methylborate anion $[MeB(C_6F_5)_3]^-$ ($\Delta\delta(p,m\text{-F}) = 2.64$) and cationic zirconium species (Scheme 6). On the basis of ^{1}H, ^{13}C, COSY, and HSQC NMR experiments, the cationic moiety is present as two isomers, with ZrMe resonances at δ 1.68/66.86 and 1.52/68.69 ppm (^{1}H/^{13}C) for the major and minor species, respectively (approximately 5:3 ratio). We have been unable to grow crystals of this compound. However, assuming that **4b** has a square pyramidal structure analogous to **5a**, the two species observed in solution are tentatively assigned as *cis* and *trans* isomers (with respect to the position of the Ar and Ar′ substituents relative to each other).

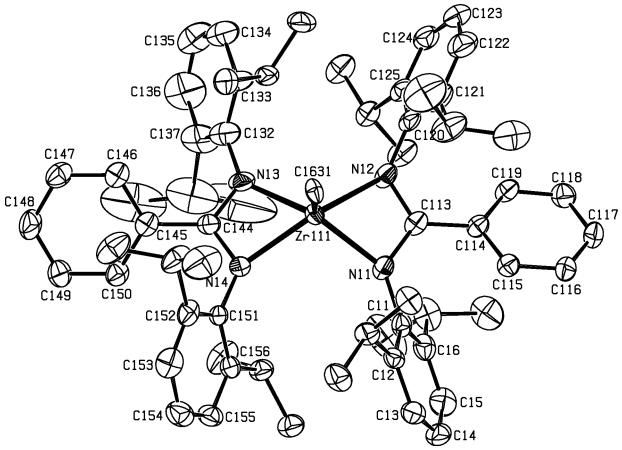

Figure 6. Molecular structure of [(**A**)$_2$ZrMe][B(C$_6$F$_5$)$_4$] (**5a**, major fraction) showing 50% probability ellipsoids. The B(C$_6$F$_5$)$_4$ anion and labels of the isopropyl groups are omitted for clarity.

The reactivity of group 4 cationic metal alkyl complexes toward unsaturated substrates usually proceeds by migratory insertion after coordination of the substrate to the metal on a vacant site located *cis* relative to the alkyl moiety. Reactivity studies of **4a** and **5a** suggest that such a site is lacking, which appears consistent with the solid state structure of the cation in **5a**. Thus, **4a** is unreactive toward CO (1 bar, 3 days at room temperature), whereas cationic zirconocene alkyl derivatives readily insert CO.[33] It also does not react with H_2 (ca. 4 bar, 24 h at room temperature), while [(R$_2$C$_5$H$_3$)ZrH][MeB(C$_6$F$_5$)$_3$] can conveniently be prepared by hydrogenolysis of [(R$_2$C$_5$H$_3$)ZrMe][MeB(C$_6$F$_5$)$_3$].[34] Furthermore, when an NMR tube containing a C_6D_6Br solution of **4a** is pressurized with 1 bar of ethylene, no reaction takes place, and there is no indication of any interaction of the cation with the olefin (based on NMR spectroscopy). Attempted ethylene polymerization runs with **2a**/[PhNMe$_2$H][B(C$_6$F$_5$)$_4$] in a 50 mL glass miniautoclave (toluene solvent, 5 bar ethylene, 50 °C) also showed no activity. In contrast, **2b**/[PhNMe$_2$H][B(C$_6$F$_5$)$_4$] does polymerize ethylene under these conditions, albeit with rather low activity (0.97 and 0.71 kg·mol^{-1}·bar^{-1}·h^{-1} for 1 and 2 h runs, respectively). Preliminary GPC analysis of the polymer formed by **2b**/[PhNMe$_2$H][B(C$_6$F$_5$)$_4$] shows a molecular weight distribution that is (at least) bimodal (peak top $M_w \approx$ 10.000 and 65.000 for 1 h run) and that could be related to the presence of two isomers observed in C_6D_5Br

(32) Horton, A. D.; De With, J.; Van der Linden, A. J.; Van de Weg, H. *Organometallics* **1996**, *15*, 2672.
(33) (a) Jordan, R. F.; Dasher, W. E.; Echols, S. F. *J. Am. Chem. Soc.* **1986**, *108*, 1718. (b) Guo, Z. Y.; Swenson, D. C.; Guram, A. S.; Jordan, R. F. *Organometallics* **1994**, *13*, 766.
(34) Yang, X. M.; Stern, C. L.; Marks, T. J. *Angew. Chem., Int. Ed.* **1992**, *31*, 1375.

solution. For a zirconium complex with a bianiline-based N_4-donor ligand, the lack of polymerization activity was ascribed to the high barrier for interconversion from the inactive *trans* to the active *cis* isomer.[18] The same rationale could apply also for the cationic bisamidinate Zr−Me species **4a** and **5a**, where a twist of the two amidinate ligands to accommodate an incoming ligand in *cis* position relative to the Zr−Me bond may be energetically prohibitive.[35]

Conclusions

From the behavior of the bisamidinate zirconium complexes with the sterically encumbered amidinate ligand $[PhC(NAr)_2]^-$ (Ar = 2,6-^{i}Pr$_2$C$_6$H$_3$, **A**) it appears that the steric interactions of the 2,6-^{i}Pr$_2$C$_6$H$_3$ substituents exert a very strong influence. It seems that the most favorable way to accommodate these ligands is to arrange the aryl substituents in a helically twisted fashion around an essentially planar arrangement of the four nitrogen atoms. This leads to an unprecedented *trans*-(**A**)$_2$ZrCl$_2$ geometry in **1a**. Although the (electronically preferred) *cis*-(**A**)$_2$ZrX$_2$ geometry is also accessible (as evidenced by the X = Me derivative **2a** and its reaction products with H_2), the preference for a planar arrangement of the two **A** ligands appears to lead to an unusual suppression of reactivity in the five-coordinate, 10 valence electron cationic alkyl species $[(\mathbf{A})_2ZrMe]^+$ present in **4a** and **5a**. The observation that the reactivity of the Zr−Me moiety in these cationic bisamidinate complexes may be gradually restored by reduction of the steric demand of one of the substituents on the amidinate ligand may point to possibilities to study the development of (catalytic) reactivity of these species as a function of gradual decrease in ligand steric demand.

Experimental Section

General Considerations. All manipulations were carried out under nitrogen atmosphere using standard glovebox, Schlenk, and vacuum-line techniques. Toluene, hexane, and pentane (Aldrich, anhydrous, 99.8%) were passed over columns of Al_2O_3 (Fluka), BASF R3-11-supported Cu oxygen scavenger, and molecular sieves (Aldrich, 4 Å). Diethyl ether (Aldrich, anhydrous, 99.8%) was dried over Al_2O_3 (Fluka). All solvents were degassed prior to use and stored under nitrogen. Deuterated solvents were vacuum transferred from Na/K alloy (C_6D_6, C_7D_8; Aldrich) or from CaH_2 (C_6D_5Br, Aldrich). H_2 (AGA, 99.9%) and D_2 (Praxair) were passed over a column of $LiAlH_4$ prior to use. $ZrCl_4$ (Aldrich), MeLi (1.5 M in Et_2O, Aldrich), ^{n}BuLi (2.5M in hexanes, Acros Organics), and $[PhNMe_2H][B(C_6F_5)_4]$ (Asahi Glass Company) were used as received. $LiCH_2SiMe_3$,[36] *N*,*N*′-bis(2,6-diisopropylphenyl)benzamidine (H**A**),[11a] *N*-(2,6-diisopropylphenyl)-*N*′-(2,6-dimethylphenyl)benzamidine (H**B**),[10] and $B(C_6F_5)_3$[37] were synthesized according to published procedures. Synthesis of the photosensitive zirconium alkyls was performed with exclusion of light by wrapping the reaction vessels in black plastic bags. NMR spectra were recorded on Varian Gemini 200, Varian VXR 300, or Varian Inova 500 spectrometers. The ^{1}H and ^{13}C NMR spectra were referenced internally using the residual solvent resonances and reported in ppm relative to TMS (0 ppm); *J* is reported in Hz. Elemental analyses were performed at the Microanalytical Department of the University of Groningen or Kolbe Microanalytical Laboratory (Mülheim an der Ruhr, Germany).

(A)$_2$ZrCl$_2$ (1a). Onto a mixture of solid H**A** (3.03 g, 6.88 mmol), $LiCH_2SiMe_3$ (0.66 g, 7.01 mmol), and $ZrCl_4$ (0.90 g, 3.86 mmol), which was frozen in liquid N_2, 50 mL of toluene was condensed. The mixture was allowed to warm to room temperature and, after stirring overnight, the solvent was pumped off. To remove residual solvent, the orange-yellow powder was stirred with 20 mL of hexane, which was removed in vacuo. The solid was extracted with hexane (4 × 75 mL). Crystallization from hexane yielded 2.32 g (2.23 mmol, 57%) of orange crystalline **1a**. ^{1}H NMR (500 MHz, C_6D_6, 25 °C): δ 7.2−6.9 (m, 16H, Ar), 6.55 (m, 6H, Ar), 4.01 (sept, J = 6.6, 4H, ^{i}Pr CH), 3.38 (sept, J = 6.3, 4H, ^{i}Pr CH), 1.49 (d, J = 6.6, 12H, ^{i}Pr Me), 1.47 (d, J = 6.6, 12H, ^{i}Pr Me), 0.83 (d, J = 6.3, 12H, ^{i}Pr Me), 0.12 (d, J = 6.3, 12H, ^{i}Pr Me). ^{13}C NMR (75.43 MHz, C_6D_6, 25 °C): δ 172.1 (s, N*C*N), 143.5 (s, *ipso*-C Ph), 142.7 (s, *ipso*-C Ar), 141.4 (s, *o*-C Ar), 131.6 (d, J = 161, Ar CH), 130.7 (d, J = 161, Ar CH), 129.4 (s, *o*-C Ar), 128.3, (d, J = 158, Ar CH), 126.5 (d, J = 159, Ar CH), 125.6 (d, J = 145, Ar CH), 123.7 (d, J = 152, Ar CH), 30.4 (d, J = 128, ^{i}Pr CH), 28.5 (d, J = 129, ^{i}Pr CH), 27.8 (q, J = 127, ^{i}Pr Me), 24.4 (q, J = 126, ^{i}Pr Me), 24.0 (q, J = 128, ^{i}Pr Me), 23.0 (q, J = 126, ^{i}Pr Me). Anal. Calcd for $C_{62}H_{78}Cl_2N_4Zr$: C, 71.50; H, 7.55; N, 5.38. Found: C, 71.39; H, 7.51; N, 5.34.

(B)$_2$ZrCl$_2$ (1b). A mixture of 1.7 g (4.4 mmol) of Li[**B**] (prepared from H**B** and ^{n}BuLi) and 50 mL of toluene was frozen in liquid N_2, and 0.66 g (2.8 mmol) of $ZrCl_4$ was added. After warming to room temperature, the mixture was stirred overnight. The solvent was removed in vacuo, and residual solvent was removed by stirring with 20 mL of hexane, which was subsequently pumped off. Extraction with pentane/toluene and cooling to −30 °C gave 1.1 g (1.2 mmol, 55%) of yellow crystalline **1b**. Crystals suitable for X-ray analysis were obtained by slowly cooling a hot hexane solution to −30 °C. ^{1}H NMR (400 MHz, C_6D_6, 25 °C): δ 7.20 (m, 10H, Ar), 6.65 (m, 12H, Ar), 3.93 (sept, J = 6.6, 4H, ^{i}Pr CH), 2.33 (s, 12 H, xy Me), 1.54 (d, J = 6.6, 12 H, ^{i}Pr Me), 0.96 (d, J = 6.7, 12H, ^{i}Pr Me). ^{13}C NMR (100.57 MHz, C_6D_6, 25 °C): δ 180.63 (s, N*C*N), 143.74 (s, Ar *o*-C), 143.71 (s, *ipso*-C), 140.50 (s, *ipso*-C), 133.75 (s, Ar *o*-C), 130.91 (d, J = 161, Ar CH), 130.55 (s, *ipso*-C), 129.62 (d, J = 162 Ar CH), 128.79 (d, overlapped, Ar CH), 127.47 (d, overlapped, Ar), 126.72 (d, J = 160, Ar CH), 125.45 (d, J = 159, Ar CH), 124.56 (d, J = 156, Ar CH), 28.95 (d, J = 127, ^{i}Pr CH), 26.47 (q, J = 127, ^{i}Pr Me), 23.86 (q, J = 127, ^{i}Pr Me), 19.81 (q, J = 126, xy Me). ^{1}H NMR (500 MHz, toluene-d_8, −90 °C): δ 7.4−6.1 (br m, 22H, Ar), 4.37 (br, 2H, ^{i}Pr CH), 3.57 (br, 2H, ^{i}Pr CH), 3.09 (br, 6H, xy-Me), 1.79 (br, 6H, ^{i}Pr Me), 1.64 (br, 6H, xy Me), 1.41 (br, 12H, ^{i}Pr Me), 0.21 (br, 6H, ^{i}Pr Me). Anal. Calcd for $C_{54}H_{62}Cl_2N_4Zr$: C, 69.80; H, 6.73; N, 6.03. Found: C, 69.90; H, 6.79; N, 5.88.

(A)$_2$ZrMe$_2$ (2a). MeLi (1.5 mmol, 1.5 M solution in Et_2O) was added to a solution of **1a** (0.65 g, 0.62 mmol) in 50 mL of Et_2O at room temperature in the dark. The mixture was stirred in the dark for 5 h, during which time the color of the solution changed from yellow to light greenish. After removal of the solvent in vacuo, residual solvent was removed by stirring the mixture twice with 10 mL of pentane, which was subsequently pumped off. After extraction of the resulting solid with pentane (4 × 30 mL) and subsequent drying in vacuo, 0.39 g (0.40 mmol, 63%) of off-white/light greenish **2a** was obtained as a powder. ^{1}H NMR (500 MHz, toluene-d_8, −30 °C): δ 6.45−7.25 (m, 22H, Ar), 4.00 (br, 4H, ^{i}Pr CH), 3.35 (br, 4H, ^{i}Pr CH), 1.61 (br d, J = 6.4, 12H, ^{i}Pr Me), 1.44 (br d, J = 6.4, 12H, ^{i}Pr Me), 1.34 (s, 6H, Zr Me), 0.75 (br d, 12H, ^{i}Pr Me), 0.46 (br d, J = 6.3, 12H, ^{i}Pr Me). ^{13}C NMR (125.89 MHz, toluene-d_8, −30 °C): δ 180.09 (s, N*C*N), 143.13 (s, *ipso*-C Ph), 143.05 (s, *ipso*-C Ar), 142.92 (s, *ipso*-C Ar), 131.14 (d, J = 160,

(35) (a) Vyboishchikov, S. F.; Musaev, D. G.; Froese, R. D. J.; Morokuma, K. *Organometallics* **2001**, *20*, 309. (b) Ramos, J.; Cruz, V.; Muñoz-Escalona, A.; Martínez-Salazar, J. *Polymer* **2001**, *42*, 7275.

(36) Negishi, E.; Swanson, D. R.; Rousset, C. J. *J. Org. Chem.* **1990**, *55*, 5406.

(37) Pohlmann, J. L.; Brinckma, F. E. *Z. Naturforsch. B* **1965**, *B 20*, 5.

Ar CH), 130.49 (s, *o*-C Ar)*, 130.04 (d, $J = 161$, Ar CH), 129.10 (d, $J = 156$, Ar CH), 128.17 (d, $J = 159$, Ar CH), 126.94 (d, $J = 163$, Ar CH), 125.58 (d, $J = 158$, Ar CH), 125.33 (d, $J = 158$, Ar CH), 57.51 (q, $J = 116$, Zr Me), 29.36 (d, $J = 131$, ^{i}Pr CH), 28.24 (d, $J = 131$, ^{i}Pr CH), 25.81 (q, $J = 126$, ^{i}Pr Me), 25.50 (q, $J = 126$, ^{i}Pr Me), 25.11 (q, $J = 124$, ^{i}Pr Me), 23.85 (q, $J = 124$, ^{i}Pr Me). *A second resonance for the *o*-C Ar could not be identified; perhaps it is obscured by the solvent resonances. ^{1}H NMR (500 MHz, toluene-d_8, 80 °C): δ 6.95−7.15 (m, 16H, Ar), 6.62 (m, 6H, Ar), 3.65 (br, 8H, ^{i}Pr CH), 1.25 (s, 6H, Zr Me), 1.14 (br, 24H, ^{i}Pr Me), 0.92 (br, 24H, ^{i}Pr Me). Anal. Calcd for $C_{64}H_{84}N_4Zr$: C, 76.82; H, 8.46; N, 5.60. Found: C, 76.71; H, 8.54; N, 5.58.

(B)$_2$ZrMe$_2$ (2b). A solution of 500 mg of **1b** (0.54 mmol) in 50 mL of Et_2O was cooled to −15 °C, and 0.85 mL of MeLi (1.36 mmol, 1.6 M solution in Et_2O) was added in the dark. After stirring at −15 °C for 15 min, the mixture was allowed to warm to room temperature and was stirred overnight. Removal of volatiles gave a brownish solid, from which residual Et_2O was removed by stirring with 10 mL of pentane and subsequent evaporation in vacuo. The solid was extracted with pentane. The resulting solution was concentrated and stored at −78 °C, which yielded 310 mg of yellow crystalline **2b** (0.35 mmol, 65%). ^{1}H NMR (400 MHz, C_6D_6, 25 °C): δ 7.22 (m, 10H, Ar), 6.67 (m, 12H, Ar), 3.87 (sept, $J = 6.7$, 4H, ^{i}Pr CH), 2.18 (s, 12H, xy Me), 1.44 (d, $J = 6.6$, 12H, ^{i}Pr Me), 1.31 (s, 6H, Zr Me), 0.98 (d, $J = 6.7$, 12H, ^{i}Pr Me). ^{13}C NMR (100.57 MHz, C_6D_6, 25 °C): δ 179.83 (s, N*C*N), 144.67 (s, *ipso*-C), 143.54 (s, Ar *o*-C), 141.95 (s, *ipso*-C), 133.14 (s, Ar *o*-C), 131.88 (s, *ipso*-C), 130.19 (d, $J = 161$, Ar CH), 129.50 (d, $J = 161$, Ar CH), 128.52 (d, overlapped, Ar CH), 127.38 (d, $J \approx 160$, Ar CH), 125.88 (d, $J \approx 154$, Ar CH), 124.39 (d, $J \approx 154$, Ar CH), 124.37- (d, $J \approx 154$, Ar CH), 53.23 (q, $J = 116$, Zr Me), 28.63 (d, $J = 126$, ^{i}Pr CH), 26.20 (q, $J = 126$, ^{i}Pr Me), 24.01 (q, $J = 125$, ^{i}Pr Me), 19.75 (q, $J = 126$, xy Me). Anal. Calcd for $C_{56}H_{68}N_4Zr$: C, 75.71; H, 7.71; N, 6.31. Found: C, 75.56; H, 7.63; N 6.18.

NMR Tube Scale Synthesis of {PhC(NAr)[NC$_6$H$_3$(^{i}Pr)-(CHMeCH$_2$)]}$_2$Zr (3a). A solution was made of **2a** (33.8 mg, 33.8 μmol) and 0.4 mL of toluene-d_8. The greenish solution was transferred to an NMR tube (equipped with a Teflon stopcock) and warmed to 50 °C in the dark. For 3 weeks, the solution was monitored by ^{1}H and ^{13}C NMR spectroscopy. Complex **2a** is fully converted within this time to a mixture of two isomers (*S*,*R*:*S*,*S* = 2:1) of **3a**. Major product (C_1 symmetric, *S*,*R* diastereomer): ^{1}H NMR (500 MHz, toluene-d_8, 25 °C) δ 7.2−6.5 (m, Ar), 4.27 (sept, $J = 7.0$, ^{i}Pr CH), 4.15 (sept, $J = 6.8$, ^{i}Pr CH), 3.83 (m, C*H*MeCH$_2$), 3.78 (m, C*H*MeCH$_2$), 3.11 (sept, $J = 6.9$, ^{i}Pr CH), 3.07 (sept, $J = 6.9$, ^{i}Pr CH), 2.95 (sept, $J = 6.9$, ^{i}Pr CH), 2.81 (sept, $J = 6.9$, ^{i}Pr CH), 2.51 (dd, $^1J_{HH} = 13.7$, $^3J_{HH} = 4.9$, CHMeC*H*H), 2.30 (d, $^1J_{HH} = 13.1$, CHMeC*H*H), 1.97 (d, $J = 7.1$, CH*Me*CH$_2$), 1.64 (d, $J = 7.1$, ^{i}Pr Me), 1.59 (br d, CH*Me*CH$_2$), 1.56 (d, $J = 7.0$, 2 × ^{i}Pr Me), 1.54 (d, overlapping, CHMeCH*H*), 1.49 (d, $J = 6.6$, ^{i}Pr Me), 1.33 (d, $^1J_{HH} = 13.7$, CHMeCH*H*), 1.24 (d, $J = 6.7$, ^{i}Pr Me), 1.21 (d, $J = 6.7$, ^{i}Pr Me), 0.32 (d, $J = 7.0$, ^{i}Pr Me), 0.25 (d, $J = 6.8$, ^{i}Pr Me), 0.18 (d, $J = 6.8$, ^{i}Pr Me), 0.13 (d, $J = 6.8$, ^{i}Pr Me), 0.04 (d, $J = 6.8$, ^{i}Pr Me), −0.01 (d, $J = 6.7$, ^{i}Pr Me). Minor product (C_2 symmetric, *S*,*S* diastereomer): δ 7.2−6.5 (m, Ar), 4.22 (sept, $J = 7.0$, ^{i}Pr CH), 3.79 (m, C*H*MeCH$_2$), 3.05 (sept, $J = 6.9$, ^{i}Pr CH), 2.78 (sept, $J = 6.9$, ^{i}Pr CH), 2.27 (d, $^1J_{HH} = 12.6$, CHMeC*H*H), 1.59 (br d, CH*Me*CH$_2$), 1.56 (d, $J = 7.0$, 2 × ^{i}Pr Me), 1.50 (d, overlapping, CHMeCH*H*), 1.21 (d, $J = 6.7$, ^{i}Pr Me), 0.30 (d, $J = 7.0$, ^{i}Pr Me), 0.09 (d, $J = 6.5$, ^{i}Pr Me), 0.03 (d, $J = 6.8$, ^{i}Pr Me). ^{13}C NMR of the mixture of isomers (125.89 MHz, toluene-d_8, 25 °C): δ 174.67 (s, N*C*N), 174.27 (s, N*C*N), 172.84 (s, N*C*N), 144.69, 144.67, 144.37, 143.88, 143.47, 143.38, 143.36, 143.31, 143.25, 143.21, 142.41, 142.01, 141.72, 141.53, 141.18, 140.58, 140.32, 140.27, 140.16 (all s, Ar C), 131−121 (overlapping, Ar), 85.40 (t, $J = 116$, CHMe*C*H$_2$), 84.85 (t, $J = 116$, CHMe*C*H$_2$), 83.89 (t, $J = 116$, CHMe*C*H$_2$), 43.91 (d, $J = 127$, ^{i}Pr CH), 37.42 (d, $J = 122$, ^{i}Pr CH), 37.09 (d, $J = 122$, ^{i}Pr CH), 29.25, 29.18, 29.12, 28.63, 28.60, 28.49, 28.46, 28.39, and 28.24 (overlapping d, ^{i}Pr CH), 26.74, 26.39, 26.33, 25.04, 24.90, 24.86, 24.66, 24.61, 24.38, 24.14, 23.90, 23.55, 22.93, 22.91, 22.78, 21.82, 21.77, and 21.57 (overlapping q, ^{i}Pr Me). Assignment was aided by HSQC and ^{1}H,^{1}H-COSY NMR spectroscopy.

{PhC(NAr)[NC$_6$H$_3$(^{i}Pr)(CHMeCH$_2$)]}$_2$Zr (3a). A solution was made of **2a** (107 mg, 0.107 mmol) in 10 mL of toluene. After stirring for 3 weeks at 50 °C in the dark, the solvent was removed in vacuo, resulting in 78 mg of **3a** (0.0805 mmol, 76%). ^{1}H and ^{13}C NMR spectra are identical to those reported for the NMR tube reaction (vide supra), with a somewhat different ratio (*S*,*S*:*S*,*R* ≈ 1:2) of the two isomers. Recrystallization from benzene/pentane gave analytically pure material. Anal. Calcd for $C_{62}H_{76}N_4Zr \cdot 0.5(C_6H_6) \cdot 0.5(C_5H_{12})$: C, 77.68; H, 8.21; N, 5.37. Found: C, 77.50; H, 8.15; N, 5.47.

Reaction of 2a with B(C$_6$F$_5$)$_3$ on NMR Tube Scale. To solid $B(C_6F_5)_3$ (6.0 mg, 11.7 μmol) was added a solution of **2a** (11.7 mg, 11.7 μmol) in 0.4 mL of C_6D_5Br. The resulting yellow solution was transferred to an NMR tube (equipped with Teflon stopcock) and measured immediately. NMR data support the quantitative formation of [(**A**)$_2$ZrMe][MeB(C$_6$F$_5$)$_3$] (**4a**). ^{1}H NMR (200 MHz, C_6D_5Br, 25 °C): δ 6.65−7.25 (m, 22H, Ar), 2.99 (sept, $J = 6.5$, 2H, ^{i}Pr CH), 2.64 (m, 4H, ^{i}Pr CH), 2.45 (sept, $J = 6.6$, 2H, ^{i}Pr CH), 1.72 (s, 3H, ZrMe), 1.43 (d, $J = 6.5$, 6H, ^{i}Pr Me), 1.14 (br, 3H, BMe), 1.07 (ps t, $J = 5.9$, 12H, ^{i}Pr Me), 0.93 (d, $J = 6.5$, 6H, ^{i}Pr Me), 0.60 (d, $J = 6.4$, 6H, ^{i}Pr Me), 0.26 (ps t, $J = 7.8$, 12H, ^{i}Pr Me), −0.05 (d, $J = 6.4$, 6H, ^{i}Pr Me). ^{19}F NMR (188.15 MHz, C_6D_5Br, 25 °C): δ −133.12 (d, $J = 23.7$, *o*-F), −165.01 (t, $J = 20.8$, *p*-F), −167.44 (t, $J = 22.1$, *m*-F), $\Delta\delta(p,m\text{-F}) = 2.43$.

[(A)$_2$ZrMe][MeB(C$_6$F$_5$)$_3$] (4a). In the glovebox, a solution was made of 20 mg of **2a** (20.0 μmol) in 2 mL of cyclohexane. This was added to a solution of 10.3 mg of $B(C_6F_5)_3$ (20.0 μmol) in 1.5 mL of cyclohexane, and after standing over the weekend the clear supernatant was decanted from the resulting yellow oil. The oil was washed two times with 1.5 mL of cyclohexane and then dried in vacuo. This gave 25.3 mg (16.7 μmol, 84%) of foamy yellow **4a**. NMR spectra are identical to those described above. Anal. Calcd for $C_{82}H_{84}BF_{15}N_4Zr$: C, 65.11; H, 5.60; N, 3.70. Found: C, 65.06; H, 6.12; N, 3.32.

Reaction of 4a with CO, H$_2$, and Ethylene. Reactions were performed by attaching NMR tubes, containing solutions of **4a** in C_6D_5Br and equipped with a Teflon stopcock, to a high-vacuum line. The solutions were frozen in liquid N_2, after which amounts of gaseous reactant were added. The tubes were closed and thawed out and the reactions monitored by ^{1}H NMR spectroscopy. Neither CO, nor H_2 or ethylene showed any reactivity within 24 h at ambient temperature or 3 h at 80 °C (CO and ethylene), or 24 h at 50 °C (H_2).

Reaction of 2a with [PhNMe$_2$H][B(C$_6$F$_5$)$_4$] on NMR Tube Scale. To solid $[PhNMe_2H][B(C_6F_5)_4]$ (37.98 mg, 47.40 μmol) was added a solution of **2a** (47.5 mg, 47.5 μmol) in 0.5 mL of C_6D_5Br. The solution was transferred to an NMR tube (equipped with Teflon stopcock). After ca. 30 min the solution had turned bright yellow and was analyzed by NMR to be [(**A**)$_2$ZrMe][B(C$_6$F$_5$)$_4$] (**5a**). Removal of C_6D_5Br solvent in vacuo and addition of toluene gave a light greenish oil, from which crystals of **5a** were grown in the course of 2 days. ^{1}H NMR (300 MHz, C_6D_5Br, 25 °C): δ 6.50−7.25 (m, 22H, Ar), 3.00 (sept, $J = 6.5$, 2H, ^{i}Pr CH), 2.65 (m, 4H, ^{i}Pr CH), 2.46 (sept, $J = 6.6$, 2H, ^{i}Pr CH), 1.72 (s, 3H, Zr Me), 1.43 (d, $J = 6.5$, 6H, ^{i}Pr Me), 1.08 (ps t, $J = 7.4$, 12H, ^{i}Pr Me), 0.93 (d, $J = 6.7$, 6H, ^{i}Pr Me), 0.61 (d, $J = 6.4$, 6H, ^{i}Pr Me), 0.28 (d, $J = 6.5$, 6H, ^{i}Pr Me), 0.24 (d, $J = 6.7$, 6H, ^{i}Pr Me), −0.04 (d, $J = 6.4$, 6H, ^{i}Pr Me). Signals due to free *N*,*N*′-dimethylaniline are observed in the aromatic region and at δ 2.58 (s, 6H, PhN*Me*$_2$). ^{13}C NMR (75.4 MHz, C_6D_5Br, 25 °C): δ 176.78 (s, N*C*N), 148.74 (d, $J_{CF} = 242$, *o*-CF), 142.46 (s, Ar C), 141.12 (s, Ar C), 140.30 (s, Ar C), 140.16 (s, Ar C), 139.17 (s, Ar C), 138.52 (d, $J_{CF} = 246$, *p*-CF), 137.41 (s, Ar C), 136.65 (d, $J_{CF} = 247$, *m*-CF), 133.21 (d, $J = 163$, Ar CH), 131.45 (d, $J = 162$, Ar CH), 128.83 (d, J

Table 5. Crystallographic Data for $(A)_2ZrCl_2$ (1a), $(B)_2ZrCl_2$ (1b), $(A)_2ZrMe_2$ (2a), and $(B)_2ZrMe_2$ (2b)

	1a	1b	2a	2b
chem formula	$C_{62}H_{78}Cl_2N_4Zr$	$C_{54}H_{62}Cl_2N_4Zr$	$C_{64}H_{84}N_4Zr$	$C_{56}H_{68}N_4Zr$
M_r	1041.46	929.20	1000.62	888.40
cryst syst	tetragonal	tetragonal	monoclinic	tetragonal
color, habit	orange, block	yellow, block	yellow, platelet	light yellow, block
size (mm)	0.30 × 0.28 × 0.20	0.20 × 0.12 × 0.07	0.25 × 0.23 × 0.04	0.21 × 0.10 × 0.08
space group	$P4_32_12$	$P4_2/n$	$P2_1/c$	$P4_2/n$
a (Å)	13.768(1)	16.4278(7)	23.088(1)	16.490(1)
b (Å)			19.109(1)	
c (Å)	31.015(3)	20.6648(9)	26.146(2)	20.765(1)
α (deg)				
β (deg)			98.486(1)	
γ (deg)				
V (Å^3)	5879.1(8)	5576.9(4)	11409.0(12)	5646.4(6)
Z	4	4	8	4
ρ_{calc} (g·cm^{-3})	1.177	1.107	1.165	1.045
μ(Mo Kα) (cm^{-1})	3.17	3.27	2.34	2.29
F(000)	2208	1952	4288	1888
temp (K)	293(1)	100(1)	100(1)	100(1)
θ range (deg)	2.19−27.55	2.33−26.37	2.20−25.03	2.32−25.68
data collected (h,k,l)	−17:17, −17:17, −40:40	−14:14, −20:20, −25:25	−27:27, −22:22, −31:29	−20:20, −19:20, −25:25
min. and max. transm	0.9108, 0.9392	0.9214, 0.9774	0.912, 0.991	0.9037, 0.9819
no. of rflns collected	51 500	53 327	81 036	42 600
no. of indpndt reflns	6754	5694	20 134	5372
no. of obsd reflns	4827 ($F_o \geq 4\sigma(F_o)$)	3997 ($F_o \geq 4\sigma(F_o)$)	10 928 ($F_o \geq 4\sigma(F_o)$)	3633 ($F_o \geq 4\sigma(F_o)$)
$R(F)$ (%)	4.03	5.07	8.43	5.86
$wR(F^2)$ (%)	10.30	14.01	26.58	17.19
GooF	1.012	0.988	1.015	1.120
weighting a,b	0.0587, 0.1397	0.0849, 0.0	0.1544, 5.1039	0.0726, 9.4836
no. of params refined	449	400	1279	283
min., max. resid dens	−0.2, 0.35(4)	−1.76, 0.48(9)	−0.8, 6.8(1)	−0.6, 1.3(1)

= 161, Ar CH), 128.31 (d, J = 162, Ar CH), 128.25 (d, J = 163, Ar CH), 126.14 (d, J = 160, Ar CH), 125.83 (d, J = 159, Ar CH), 124.49 (d, J = 158, Ar CH), 68.77 (q, J = 119, Zr Me), 37.08 (d, J = 117, ^{i}Pr CH), 30.37 (d, J = 122, ^{i}Pr CH), 28.92 (d, J = 126, ^{i}Pr CH), 28.74 (d, J = 123, ^{i}Pr CH), 26.17 (q, J = 126, ^{i}Pr Me), 24.65 (q, J = 128, ^{i}Pr Me), 2 × 23.77 (q, J = 124, ^{i}Pr Me), 22.36 (q, J = 124, ^{i}Pr Me), 22.30 (q, J = 121, ^{i}Pr Me), 21.31 (q, J = 127, ^{i}Pr Me), 20.65 (q, J = 126, ^{i}Pr Me). Signals due to free *N*,*N*′-dimethylaniline are observed at δ 129.87 (d, J = 161, $PhNMe_2$), 125.36 (s, $PhNMe_2$), 117.58 (d, J = 160, $PhNMe_2$), 113.29 (d, J = 156, $PhNMe_2$), 40.64 (q, J = 135, $PhNMe_2$). ^{19}F NMR (188.15 MHz, C_6D_5Br, 25 °C): δ −132.63 (br d, *o*-F), −162.81 (t, J = 20.8, *p*-F), −166.67 (br t, *m*-F).

Reaction of 2b with $B(C_6F_5)_3$ on NMR Tube Scale. A solution of 8.2 mg of **2b** in 0.5 mL of C_6D_5Br was added to solid $B(C_6F_5)_3$ (1 equiv), and the resulting yellow solution was transferred to an NMR tube (equipped with a Teflon stopcock). The ^{1}H NMR spectrum is broad at room temperature, and the sample was cooled in the NMR spectrometer to −30 °C. ^{1}H, ^{13}C, COSY, and HSQC NMR experiments at that temperature are consistent with the formation of two isomers of the ionic complex $[(\mathbf{B})_2ZrMe][MeB(C_6F_5)_3]$ (**4b**). Major isomer: ^{1}H NMR (500 MHz, C_6D_5Br, −30 °C) δ 7.15−6.55 (m, Ar), 3.11 (br, ^{i}Pr CH), 2.60 (br, ^{i}Pr CH), 1.91 (s, xy Me), 1.68 (s, ZrMe), 1.67 (s, xy Me), 1.12 (br, 2 × ^{i}Pr Me), 0.84 (br, ^{i}Pr Me), 0.68 (br, ^{i}Pr Me). ^{13}C NMR (125.89 MHz, C_6D_5Br, −30 °C): δ 178.16 (*NCN*), 66.86 (ZrMe), 30.31 (^{i}Pr CH), 29.97 (^{i}Pr CH), 28.53 (^{i}Pr Me), 22.68 (2 × ^{i}Pr Me), 21.34 (^{i}Pr Me), 19.39 (xy Me), 18.63 (xy Me). Minor isomer: ^{1}H NMR (500 MHz, C_6D_5Br, −30 °C) δ 7.15−6.55 (m, Ar), 3.05 (br, ^{i}Pr CH), 2.56 (br, ^{i}Pr CH), 1.83 (s, xy Me), 1.52 (s, ZrMe), 1.46 (s, xy Me), 1.45 (br, ^{i}Pr Me), 1.01 (br, ^{i}Pr Me), 0.62 (br, ^{i}Pr Me), 0.16 (br, ^{i}Pr Me). ^{13}C NMR (125.89 MHz, C_6D_5Br, −30 °C): δ 176.00 (*NCN*), 68.69 (ZrMe), 36.57 (^{i}Pr CH), 28.88 (^{i}Pr CH), 25.00 (^{i}Pr Me), 23.80 (^{i}Pr Me), 23.19 (^{i}Pr Me), 21.72 (^{i}Pr Me), 18.87 (xy Me), 18.06 (xy Me). Resonances in the aromatic region could not be unequivocally assigned, and some may be overlapped by solvent (δ 140.70, 140.36, 140.06, 139.73, 139.40, 139.26, 138.62, 133.59, 133.11, 129.06, 128.57, 127.60, 127.20, 126.06, 125.01, 124.65, 123.94, 122.15). Data for the $[MeB(C_6F_5)_3]$ anion: ^{1}H NMR (500 MHz, C_6D_5Br, −30 °C) δ 1.27 (br, BMe). ^{13}C NMR (125.89 MHz, C_6D_5Br, −30 °C): δ 148.80 (d, J_{CF} = 238, *o*-CF), 137.71 (d, J_{CF} = 241, *p*-CF), 136.73 (d, J_{CF} = 244, *m*-CF), 11.14 (br, BMe). ^{19}F NMR (470.28 MHz, CD_2Cl_2, −20 °C): δ −132.02 (d, J = 24.4, *o*-F), −163.42 (t, J = 20.7, *p*-F), −166.06 (t, J = 22.5, *m*-F), Δδ(*p*,*m*-F) = 2.64.

X-ray Structures. Suitable crystals of **1b**, **2a**, **2b**, **3a**, and **5a** were mounted on top of a glass fiber in a drybox and transferred, using inert-atmosphere handling techniques, into the cold nitrogen stream of a Bruker SMART APEX CCD diffractometer. For **1a**, attempts to determine the crystal structure at 100 and 200 K were unsuccessful (probably due to a phase transition), and a suitable crystal was sealed inside a Lindemann glass capillary in a drybox and measured at room temperature. The final unit cell was obtained from the *xyz* centroids of 5557 (**1a**), 3307 (**1b**), 7208 (**2a**), 9171 (**2b**), 7165 (**3a**), or 8159 (**5a**) reflections after integration. Intensity data were corrected for Lorentz and polarization effects, scale variation, and decay and absorption: a multiscan absorption correction was applied, based on the intensities of symmetry-related reflections measured at different angular settings (SADABS).[38] The structures of **1a**, **2a**, **3a**, and **5a** were solved by Patterson methods, and extension of the model was accomplished by direct methods applied to difference structure factors using the program DIRDIF.[39] The structures of **1b** and **2b** were solved by direct methods with SIR-97.[40] Hydrogen atom coordinates and isotropic displacement parameters were refined freely for **1a** (except those on C(9) and C(26)) and **1b**. In all other cases, hydrogen atoms were included riding on their carrier atoms. The crystals obtained for **2a** showed weak scattering power. In the difference Fourier map two peaks of 6.78 and 6.27 e/Å^3 were observed with nearest non-hydrogen atoms C(231) (1.50 Å, isopropyl Me) and C(254) (2.28 Å, *p*-C of diisopropylphenyl group). Crystals obtained from a different

(38) Sheldrick, G. M. *SADABS* v. 2, *Multi-Scan Absorption Correction Program*; University of Göttingen: Germany, 2001.

(39) Beurskens, P. T.; Beurskens, G.; Gelder, R. de; García-Granda, S.; Gould, R. O.; Israël, R.; Smits, J. M. M. *The DIRDIF-99 Program System*; Crystallography Laboratory, University of Nijmegen: The Netherlands, 1999.

(40) Altomare, A.; Burla, M. C.; Camalli, M.; Cascarano, G. L.; Giacovazzo, C.; Guagliardi, A.; Moliterni, A. G. G.; Polidori, G.; Spagna, R. *J. Appl. Crystallogr.* **1999**, *32*, 115.

Table 6. Crystallographic Data for {PhC(NAr)[NC$_6$H$_3$(^{i}Pr)(CHMeCH$_2$)]}$_2$Zr (3a) and [(A)$_2$ZrMe][B(C$_6$F$_5$)$_4$] (5a)

	3a	5a
chem formula	$(C_{62}H_{76}N_4Zr)\cdot 0.5(C_6D_6)\cdot 0.5(C_5H_{12})$	$[C_{63}H_{81}N_4Zr]^+\cdot[C_{24}F_{20}]^-$
M_r	1046.69	1664.63
cryst syst	monoclinic	orthorhombic
color, habit	yellow, block	yellow, block
size (mm)	0.16 × 0.14 × 0.10	0.38 × 0.22 × 0.19
space group	*C*2/*c*	*Pbca*
a (Å)	46.293(4)	21.8555(8)
b (Å)	13.983(1)	24.9323(9)
c (Å)	18.539(2)	29.067(1)
β (deg)	94.771(1)	
V (Å^3)	11959.0(19)	15838.8(10)
Z	8	8
ρ_{calc} (g·cm^{-3})	1.163	1.396
μ(Mo K$\bar{\alpha}$) (cm^{-1})	2.26	2.34
F(000)	4464	6848
temp (K)	100(1)	100(1)
θ range (deg)	2.20−25.03	2.33−26.02
data collected (*h*,*k*,*l*)	−55:54, 0:16, 0:22	−26:26, −30:30, −34:35
min. and max. transm	0.8847, 0.9778	0.892, 0.957
no. of rflns collected	51 795	119 963
no. of indpndt reflns	10 561	15 585
no. of obsd reflns	7379 ($F_o \geq 4\sigma(F_o)$)	11992 ($F_o \geq 4\sigma(F_o)$)
R(*F*) (%)	6.20	8.59
wR(*F*^{2}) (%)	14.14	17.91
GooF	1.080	1.193
weighting *a*,*b*	0.0, 29.7352	0.0, 72.4221
no. of params refined	677	1055
min., max. resid dens	−0.62, 0.6(7)	−0.87, 1.09(8)

batch of compound showed similar problems. No satisfactory discrete (twin) model could be fitted in this density. Nevertheless, the connectivity for the non-hydrogen atoms could be unequivocally established. Crystals obtained for **3a** also showed weak scattering power. A difference Fourier synthesis indicated that C(30) partially occupied two positions, and C(39) and C(40) showed rotational disorder. These atoms were refined as occupying two positions, with the major fractions refining to a sof of 0.77 for C(30) and 0.67 for C(39) and C(40). Similar two-site occupancies for the rest of the ligand set could not be resolved, resulting in some atoms showing unrealistic displacement parameters. The solvent pentane molecule was highly disordered over a 2-fold axis, which could not be satisfactory described. For **5a**, it was clear from the difference Fourier map that the cationic part of the molecule is also present in a different orientation in the crystal lattice. The central Zr−Me moiety was found to be partly located on two sides of the plane formed by the four N atoms. This part was refined as occupying two positions, with the largest fraction, Zr(111) and C(1631), refining to a sof of 0.74. It was impossible to locate the ligand set belonging to the minor orientation, resulting in some atoms showing unrealistic displacement parameters. All refinement and geometry calculations were performed with the program packages SHELXL[41] and PLATON.[42] Crystal data and details on data collection and refinement are presented in Tables 5 and 6.

Polymerization Runs. For the polymerization experiments, the toluene solvent (Aldrich anhydrous, 99.5%) and the ethylene (AGA, polymer grade) were passed over columns of oxygen scavenger (BASF R3-11) and molecular sieves (4 Å) before being passed to the reactor. Gel permeation chromatography (GPC) analysis of the polyethylenes was carried out by A. Jekel (University of Groningen) on a Polymer Laboratories Ltd. (PL-GPC210) chromatograph using 1,2,4-trichlorobenzene (TCB) as the mobile phase at 150 °C. The samples were prepared by dissolving the polymer in the mobile phase solvent in an external oven at 0.1% (weight/volume) and were run without filtration (column: 4PL-Gel Mixed A). The molecular weight was referenced to polystyrene (M_w = 65 500, PDI = 1.02) standards. The polystyrene was used for column calibration−single point calibration for Triple Detector (RI + Visco + LS, 90°) (VISCOTEK, Software: TRISEC).

Ethylene Polymerization with 2a/[PhNMe$_2$H][B(C$_6$F$_5$)$_4$] and 2b/[PhNMe$_2$H][B(C$_6$F$_5$)$_4$]. The polymerizations were performed in a 50 mL glass miniclave (Büchi A. G., Switzerland) with a magnetic stirrer. Before use, the reactor was dried at 80 °C in a vacuum oven for at least 2 h. In a drybox, the miniclave was charged with dialkyl compound **2a** or **2b** (20 μmol) and 15 mL of toluene, and [PhNMe$_2$H][B(C$_6$F$_5$)$_4$] (20 μmol) was added. The reactor was taken out of the drybox, heated at 50 °C in an oil bath, and pressurized with 5 bar of ethylene. The pressure was kept constant during the reaction by replenishing the flow. The reaction mixture was stirred for the required reaction time and then vented. The polymer was repeatedly rinsed with acidified methanol and dried in a vacuum oven.

Acknowledgment. We thank A. Jekel for polymer GPC analysis, and the Council for Chemical Sciences of The Netherlands Foundation for Scientific Research (NWO-CW) and NRSC-Catalysis for financial support.

Supporting Information Available: Text describing the analysis of the EXSY experiments, low-temperature NMR spectra for **2a**, and details of the crystallographic study of **1a**, **1b**, **2a**, **2b**, **3a**, and **5a**. This material is available free of charge via the Internet at http://pubs.acs.org.

OM050342J

(41) Sheldrick, G. M. *SHELXL-97, Program for the Refinement of Crystal Structures*; University of Göttingen: Germany, 1997.
(42) Spek, A. L. *PLATON. Program for the Automated Analysis of Molecular Geometry (A Multipurpose Crystallographic Tool)*; University of Utrecht: The Netherlands, 2005.
(43) *SPARTAN '*02; Wavefunction Inc.: Irvine, CA, 2002.